

ROLE OF REACTIVE OXYGEN SPECIES AND ALTERED BIOCHEMICAL
PATHWAYS IN CELLULAR AGING

THESIS

Presented to the Graduate Council
of Texas State University-San Marcos
in Partial Fulfillment
of the Requirements

for the Degree

Master of SCIENCE

by

Alison Lee Russell, B.S.

San Marcos, Texas
May 2006

ACKNOWLEDGEMENTS

I would like to begin by thanking Dr. Lewis for his encouragement, guidance and patience. I have acquired more knowledge and experience more now than ever before. You are an amazing professor, advisor and great friend and I will always carry your words of wisdom wherever I go. As you say, “never give up, adjust and try again.” I wish you the best and good luck with those grants.

I would like to dedicate my thesis work to my parents. I owe my success to my family. I can not express in words my appreciation for all of your love and support. I could not be who I am today if it wasn't for my parents. I love you both and you will always be in my heart.

Last, but not least, I would like to acknowledge my love, Brian. You have been an inspiration and a real trooper. Thanks for being supportive and always pushing me to do better and strive for more. You are an amazing individual and have so much going for you. I love you and wish you the best.

TABLE OF CONTENTS

	PAGE
ACKNOWLEDGEMENTS.....	iii
LIST OF TABLES.....	v
LIST OF FIGURES.....	vi
CHAPTER	
I. INTRODUCTION.....	1
II. MATERIALS AND METHODS.....	14
III. RESULTS AND DISCUSSION.....	33
REFERENCES.....	69

LIST OF TABLES

TABLE	PAGE
1. <i>Saccharomyces cerevisiae</i> strains.....	18

LIST OF FIGURES

FIGURE	PAGE
1. Schematic of telomere replication.....	2
2. Incidence rate of cancer.....	4
3. Model of the <i>EST2</i> expression system.....	34
4. Senescence streak assay of cells <i>est2⁻</i> cells on YPGlu (rich) and synthetic (defined) media.....	36
5. Senescence assay of <i>est2⁻</i> cells grown on various concentrations of glucose.....	38
6. Senescence assay of <i>est2⁻</i> cells at various incubation temperatures.....	39
7. Senescence assay of <i>est2⁻</i> cells on the 4 th streak on rich and synthetic media.....	40
8. Effect of 3 mM FeCl ₃ , 3 mM FeCl ₃ + 0.5 mM H ₂ O ₂ and 0.5 mM H ₂ O ₂ on <i>est2⁻</i> cells.....	43
9. Effect of 0.25 mM tert-butyl hydroperoxide, 0.5 mM t-BHP and and 0.75 mM t-BHP on <i>est2⁻</i> cells.....	44
10. Effect of 0.025 mM and 0.1 mM menadione on <i>est2⁻</i> cells.....	45
11. Effect of 0.025 mM and 0.1 mM cadmium chloride on <i>est2⁻</i> cells.....	46

12. Senescence streak assay of <i>est2⁻</i> , <i>est2⁻ rad52⁻</i> and <i>est2⁻ mre11⁻</i> cells.....	48
13. Chromosomal <i>GPX3</i> disruption via homologous recombination.....	49
14. Antioxidant enzyme defense reactions with ROS.....	51
15. Conformation of <i>Nat1^r</i> gene amplification via PCR.....	52
16. Conformation of chromosomal <i>GPX3</i> and <i>CTT1</i> gene inactivation.....	53
17. Senescence assay of <i>est2⁻</i> , <i>est2⁻ gpx3⁻</i> and <i>est2⁻ ctt1⁻</i> cells.....	54
18. Senescence assay of <i>est2⁻ gpx3⁻ ctt1⁻</i> cells at 30°C and 40°C.....	56
19. Senescence assay of <i>est2⁻</i> -BY4741, <i>est2⁻ yap1⁻</i> and <i>est2⁻ yap1⁻ gpx3⁻</i> cells at 30°C.....	58
20. Senescence assay of <i>est2⁻</i> -BY4741, <i>est2⁻ yap1⁻</i> and <i>est2⁻ yap1⁻ gpx3⁻</i> cells at 40°C.....	59
21. Senescence assay of <i>est2⁻ gpx3⁻ gpx2⁻ gpx1⁻</i> at 30°C and 40°C.....	60
22. Plating efficiency of <i>est2⁻</i> cells post-senescence.....	65

CHAPTER 1

INTRODUCTION

All humans and multi-cellular organisms grow old and eventually die. As humans age, their immune systems break down, cellular chromosomes accumulate mutations and cells build up oxidation by-products. Current research is exploring why humans experience age-related diseases and whether it is possible to reverse age-related changes in physiology. Researchers hypothesize that at least part of the answer is within the ends of chromosomes.

At the ends of eukaryotic chromosomes there is a region of short repeated sequences, called the telomere. Telomeres are bound by protein complexes that form a cap which provides structural stability and protection of the ends of chromosomes against lethal rearrangements, recombination, and degradation. Mutation and/or loss of the telomere associated proteins leads to “uncapping,” loss of essential genetic information, and telomere dysfunction. Telomeres also aid in the complete replication of chromosomal DNA. During the synthesis phase (S phase) of normal replication of chromosomes, telomere DNA is normally replicated by telomerase. Telomerase is an end-specific RNA-dependent DNA polymerase that adds DNA (or nucleotides of DNA) to the ends of chromosomes during S phase. The telomerase complex consists of several protein subunits and an RNA subunit that contains the template for telomere repeat

addition of nucleotides to the 3' end of the chromosome. Telomerase extends the 3' end of a chromosome by repetitively translocating down the chromosome and elongating the telomere during each S phase (Figure 1). The enzyme is therefore required to produce telomerase to maintain telomere length and overcome the “end-replication problem” brought about by the inability of major DNA polymerases to synthesize the lagging strand during the cell cycle. Cells that lack telomerase experience progressive telomere shortening and eventual cell death.

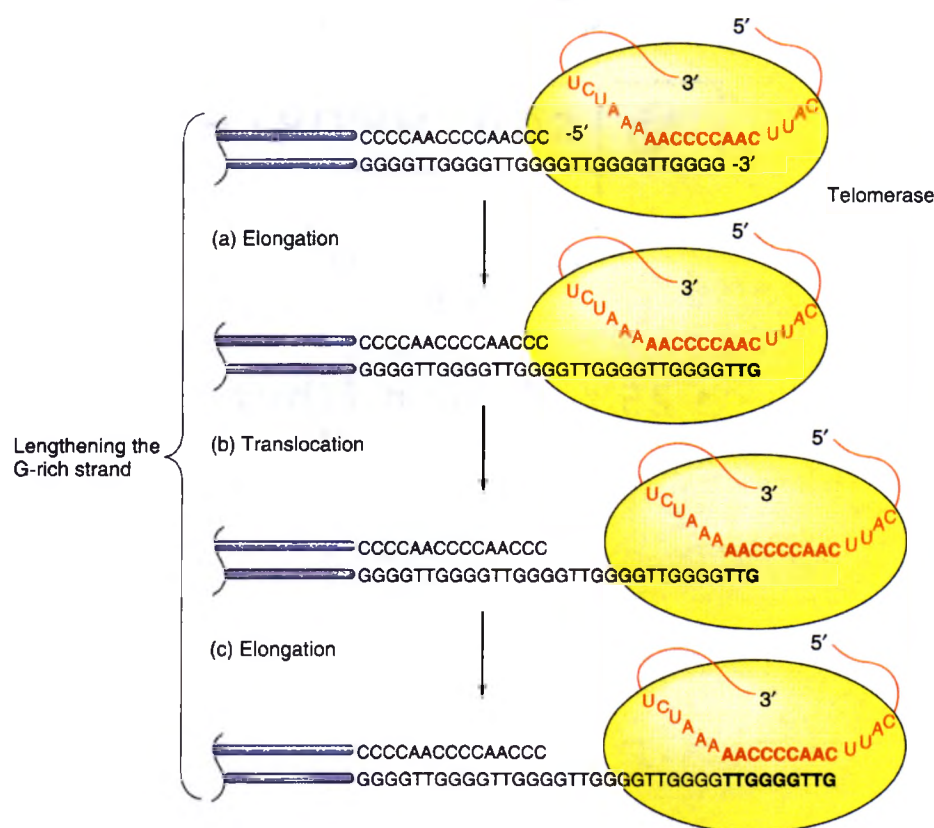


Figure 1. Schematic diagram of telomere replication by telomerase RNA.

In humans, the telomeric DNA sequence consists of a six nucleotide repeat: TTAGGG. This sequence is repeated more than a thousand times at the telomeres. Complete replication of these ends does not occur in most human somatic cells because production of telomerase is halted during embryonic development (1). Thus, as humans age, the ends of chromosomes are progressively shortened.

As stated above, telomerase is inactive in most human somatic cells. However, in over 90% of human and animal cancers, telomerase has been reactivated (2). Reactivation of telomerase is important in explaining why cancerous cells are “immortal” and divide without a finite limit. Cultured normal cells that do not express active telomerase replicate approximately fifty to sixty times during which they begin to experience chromosome instability and cellular senescence (cell death). Research studies have recognized that changes in telomere length have also been associated with various disease processes including neurodegenerative disorders (3).

Other reports have suggested that shortened telomeres actually promote chromosome instability and carcinogenesis. For example, Meeker *et al.* identified the formation of shortened dysfunctional telomeres as an early step in the development of prostate cancer (4). Shortened telomeres and an increased incidence of some cancers were also identified in telomerase knockout mice (5, 6). A possible explanation for increased chromosome instability caused by shortened telomeres is that the chromosome ends become uncapped and highly reactive. The loss of telomere-associated protein complexes may cause the cell to interpret broken DNA ends as a form of induced DNA damage and activate checkpoint and/or apoptosis-type responses (7-9).

The incidence of cancer increases with age, rising exponentially after the age of forty (Figure 2). As humans age and telomeres are progressively shortened, cells accumulate DNA damage and mutations that increase the incidence of cancer. As suggested by the studies of Meeker *et al.* and others, it is possible that telomere shortening plays a role in this process (4).

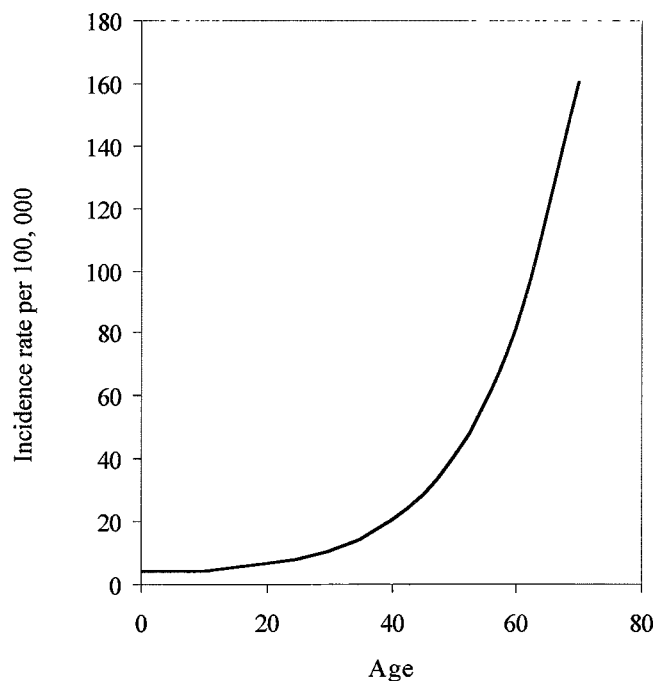


Figure 2. The incidence of most cancers show a dramatic increase with age, which is thought to be a result of increased mutation in human somatic cells

Recent studies by Cawthon *et al.* have demonstrated that individuals with shorter telomeres have a significantly higher mortality rate and accelerated aging compared to those with longer telomeres (10). It is currently unclear whether telomere shortening during human aging is simply another phenotype associated with the process or might actually determine lifespan.

Caloric restriction, oxidative stress and environmental stress are several factors that may influence the rate of telomere shortening and cell aging. Many studies using mice and rats as a model have shown that the lifespan of a mouse or rat can be increased by reducing the quantity of calorie intake by 30-40% (11). For example, one experiment (11) was conducted with two different groups of mice of various ages. The experiment monitored a control group of mice with no diet restrictions and a group on a restricted diet. The oldest mice in the control group lived 1144 days and those on a restricted caloric diet lived 100 days longer for a total of 1244 days. Results such as this have suggested that dietary changes can have an impact on cellular aging. Further experiments have revealed that, for example, limiting the quantity of amino acid intake can protect animals against age-related disease and damage (11). Caloric restriction also appears to decrease production of reactive oxygen species (ROS) during aging. An experiment investigated the effects on cells lacking an antioxidant enzyme, superoxide dismutase (SOD), in *Drosophila melanogaster* (fruit flies) (12). Results confirmed that flies lacking the antioxidant enzyme SOD reduced their lifespan by 80% when compared to wildtype *Drosophila* with SOD (12). Future experiments involve investigating the roles of ROS in aging in higher organisms.

Telomere research has also found connections between naturally occurring oxidative damage, telomere shortening and cell senescence. High levels of oxidative DNA damage can reduce chromosome stability during normal growth and can ultimately lead to chromosome loss, recombination, mutation, and or changes in gene expression. Recent experiments in normal human cells have suggested that spontaneously occurring oxidative damage may also influence the rate of telomere shortening. Oxidative damage can be induced in DNA and other macromolecules by a variety of reactive oxygen

species (ROS), such as the hydroxyl radical, superoxide anion, and peroxy radical. ROS are products of aerobic metabolism and naturally occurring free radical compounds (3). As a consequence of exposure to ROS, cells accumulate damage to chromosomal DNA, generating a variety of modified bases and deoxyribose structures (13). Oxidation also generates other DNA lesions such as single and double-strand breaks (14). Evidence suggests that guanine-rich sequences found at telomeres are more susceptible to oxidative damage than non-telomeric DNA sequences (15). 8-oxoguanine represents a DNA lesion induced by oxidative damage, specifically by hydroxyl radicals. Interestingly, telomere shortening also occurs when primary human cells are grown in culture. Primary human cells, for example, typically grow in tissue culture for approximately fifty divisions, during which time they experience morphological and biochemical changes that lead to senescence. Chen *et al.* proposed that senescence of human fibroblast cells in culture is correlated with increased levels of oxidative DNA damage (16). Experiments confirmed that senescent human fibroblast cells produced higher levels of 8-oxoguanine (16). Current studies are exploring the mechanisms and correlations between oxidative DNA damage and telomere shortening.

In addition to studies suggesting that naturally occurring oxidation processes increase the rate of senescence, exposure to exogenous pro-oxidants may also induce DNA damage and therefore increase the rate of telomere shortening by increasing levels of ROS. It has been hypothesized that oxidative DNA damage may occur preferentially at the G-rich telomere repeat sequences and affect the rate of telomere shortening. The reduction of oxygen by organic compounds is important in the generation of free radicals that can induce cellular damage. The production of ROS can be catalyzed by pro-

oxidants such as: hydrogen peroxide, iron, bleomycin, menadione or cadmium.

Hydrogen peroxide generates both peroxy and hydroxyl radicals. For example, the reduction of hydrogen peroxide, referred to as the Fenton reaction, generates hydroxyl radicals via a higher oxidation state of iron. On the other hand, excessive levels of transition metals alone are toxic to cells. Bleomycin is another pro-oxidant and it binds iron (Fe) and oxygen to form free radical complexes that induce DNA single and double-strand breaks. Menadione also generates ROS, especially superoxide radicals, and is useful in studying the effects of ROS on cellular function. Cadmium (Cd) is a well known carcinogen that induces DNA damage. Evidence suggests that the toxicity and recombinagenic activity of cadmium is caused by oxidative stress in yeasts (17).

Cells can respond to free radicals via several antioxidant defense mechanisms that can reduce oxidative damage. Enzymes such as catalase, superoxide dismutase (SOD) and glutathione peroxidase (GPX) are effective defense mechanisms against ROS. When *Caenorhabditis elegans* (nematode worms) were treated with synthetic superoxide dismutase and catalase mimetics, their life-spans were successfully increased (18). In another study, transgenic fruitflies, *Drosophila melanogaster*, expressed high levels of superoxide dismutase and catalase simultaneously. Orr and Sohal (19) concluded that the life-span of *Drosophila* was significantly increased while oxidative DNA damage decreased. These results have led to the proposal that aging in lower organisms is modulated by ROS (12). Other antioxidant defense molecules or chemicals include glutathione (GSH) and vitamins E and C which are non-enzymatic molecules that can bind and neutralize oxidative radicals (20). An oxidation-resistant type of ascorbic acid (vitamin C), Asc-2-O-phosphate, is an antioxidant that reduced telomere shortening rates

by ~ 52-62 % in cultured human cells (21). In conditions of oxidative stress in yeast cells, the naturally occurring metabolite lipoic acid has been shown to protect against hydrogen peroxide (22). Lastly, a spin-trapping agent, α -phenyl-t-butyl nitron (PBN), can act as an antioxidant by trapping intracellular radical species and preventing them from interacting with cellular macromolecules (16). Ames' group demonstrated that PBN was capable of extending the replicative life span of human fibroblasts and delaying senescence. Several of the above antioxidants are important in the natural defense mechanisms of organisms, either eliminating or reducing oxidation at the cellular level.

Similar telomere loss and senescence phenotypes are observed in other cultured eukaryotic cells, including the widely studied model eukaryote *Saccharomyces cerevisiae* (budding yeast) (23). An advantage of using this organism to study aging is that cell senescence (about sixty doublings) occurs over approximately one week versus months in cultured human cells and can therefore facilitate studies.

Yeast telomeres have approximately 300-400 base pairs (bp) of a $TG_{(1-3)}$ repeat sequence that are maintained, as in humans, by telomerase. In yeast cells, the telomerase complex is composed of four major protein subunits (Est1, Est2, Est3 and Cdc13) and an RNA subunit (*TLC1*) that synthesizes new DNA at the ends of chromosomes. Mutations in the *EST1*, *EST2*, *EST3* or *CDC13* genes lead to progressive telomere shortening and cellular senescence, thus mimicking telomerase-deficient human cells in culture. Est1 and Cdc13 proteins can bind to single-stranded G-rich telomere regions (24, 25). Est2 is the catalytic polymerase subunit and the function of Est3 is unknown. *TLC1* encodes the RNA template component of the telomerase complex. The yeast telomerase complex functions similarly to that of normal human cells in culture, given that telomeres will

continue to shorten and the cell will eventually die after about sixty divisions if this telomerase complex is not present (e.g., after inactivation of the *EST2* gene). Rare survivor mutants are sometimes observed that have found a way to bypass senescence. These cells have increased levels of homologous recombination (exchange of genetic material) between chromosome ends to maintain telomere length in late passage cultures (26). Such survivors depend on *RAD52*-mediated recombination between telomeres in yeast cells (26).

Gene disruption and inactivation provides a means for testing and manipulating versions of an altered gene for further genetic and phenotypic analysis. The effects of inactivating genes encoding the protein subunits and/or the RNA subunit of telomerase produce a phenotype of cells with chromosome instability, G₂ phase arrest, and loss of the ability to grow after approximately sixty to seventy generations (called senescence). For example, after inactivating the *EST2* gene that encodes the polymerase subunit of telomerase, cells exhibit a senescent phenotype (loss of growth). After approximately sixty generations, the telomerase-deficient cells with *EST2* inactivated acquire increased levels of chromosome instability and can no longer grow.

When cells have acquired DNA damage or shortened telomeres, they will respond by arresting growth and activating DNA repair enzymes in G₂ phase of the cell cycle. As mentioned previously, G₂ arrest is one of several phenotypic characteristics ultimately occurring in cells that have a gene encoding a subunit of telomerase inactivated. Cell cycle checkpoint regulatory genes required for arrest after DNA damage, e.g., *MEC3* and *RAD24*, are also required for the cell cycle delay in telomerase-deficient cells suggesting that the short telomeres are recognized as DNA damage (27, 28). Enomoto *et al.* (27)

propose that a “telomere checkpoint” exists and is distinct from the normal DNA damage checkpoint. The telomere checkpoint triggers a delay in the cell cycle while activating telomerase and or other telomere repair activities when telomeres have become significantly short and lost cap function. When cells are checkpoint-deficient (e.g., the *RAD24* gene inactivated), cells can no longer efficiently arrest in G₂ and are therefore unable to pause to allow time for repair of DNA damage (28).

Cells of the budding yeast *Saccharomyces cerevisiae* express two forms of superoxide dismutase: MnSOD (encoded by *SOD2*) in the mitochondrial matrix and CuZnSOD (encoded by *SOD1*) in the cytosol, nucleus, and lysosome. These enzymes are necessary for protecting cells from oxidative damage. Catalase, on the other hand, is not essential for yeast cells under normal conditions, but is vital in the acquisition of tolerance to oxidative damage (29). Yeast encodes at least two catalase enzyme genes, *CTT1* and *CTA1*. SOD enzymes have a first line of defense that catalyzes cleavage of superoxide to H₂O₂ and water. H₂O₂ is enzymatically catabolized by catalase and several peroxidases in aerobic organisms to molecular oxygen and water (29).

Glutathione (GSH) is an abundant thiol that has been proposed to have many roles in protecting cells against the deleterious effects of ROS. Yeast cells that lack GSH are sensitive to oxidative stress induced by free radicals. GSH appears to be the primary antioxidant for protection against hydrogen peroxide (20). Studies in yeast have indicated that GSH is dependent on the redox-active sulfhydryl moiety of its cysteine residue, which acts as a free radical scavenger. Glutathione becomes oxidized directly by reaction with free radicals or in reactions catalyzed by glutathione peroxidase to form GSSH (oxidized form of GSH). Genes *GPX1*, *GPX2* and *GPX3* of *Saccharomyces*

cerevisiae encode three different glutathione peroxidases that protect yeast against hydroperoxides during oxidative stress (30). Evidence suggests that the product of *GPX3* is the most important form in the cells (3).

In response to stress conditions, the synthesis of numerous protective molecules including both the GSH/glutaredoxin and thioredoxin systems is upregulated in yeast cells. This creates the basis of an inducible adaptive response, in which cells treated with low doses of oxidation can adapt to become resistant to lethal treatment (3). In these systems of GSH and thioredoxin, stress-responsive control mechanisms have been generated which include the Yap1 and Skn7 transcriptional regulators. The synthesis and reduction of GSH have been shown to be primarily regulated by the Yap1 transcription factor (3). Studies have reported that Gpx3, one of the three glutathione peroxidase homologues described earlier, functions as a redox transducer for Yap1 (30). In addition to the GSH system, expression of thioredoxin-related genes is subject to regulation by the Yap1 and Skn7 transcriptional proteins. Yap1 regulated genes include thioredoxin peroxidases *TSA1* and *TSA2* (3). Thioredoxin peroxidases (TSA), such as cytosolic Tsa1p are involved in the reduction of H₂O₂ and alkyl hydroperoxides using hydrogens from thioredoxin, thioredoxin reductase, and NADPH. Yeast strains lacking *TSA1* are viable, but highly sensitive to oxidative stress induced by superoxide anion and peroxides (such as tert-butyl hydroperoxide) (31). As a result, the Yap1 transcriptional activator protein is required for the up-regulation of both the thioredoxin system and GSH pathways.

Sophisticated gene manipulation techniques can be utilized in the yeast *Saccharomyces cerevisiae* to carefully modulate the on/off system of telomerase in cells.

With the use of a newly developed and regulatable telomerase protein expression system, researchers can modulate expression of the polymerase subunit of telomerase (*EST2*) using a version of the yeast galactose regulatory system. A centromeric plasmid containing a *GAL1p::EST2* promoter fusion has been developed recently in the Lewis lab to permit turning off telomerase by switching cells from galactose to glucose-containing media. A new *GAL1* promoter was created by mutagenesis of the native *GAL1* promoter to identify variants with lower basal expression in the “OFF” condition. After telomerase expression is halted, cells experience changes in telomere structure, length and eventually undergo senescence.

The major goal of this project was to use this *EST2* expression system to analyze the factors that influence telomere shortening and *in vitro* aging. Such factors include the effects of caloric restriction and variation of growth temperature on cell senescence. As stated previously, oxidative stress has been shown to influence the rate of telomere shortening and cell aging in several organisms. This project investigated the effects of oxidation on the rate of telomere shortening in yeast. Furthermore, mutant cells with inactivated genes encoding enzymes needed for direct deactivation of oxidative radicals (e.g., when the catalase gene has been inactivated, the new catalase-deficient cells will have increased levels of free radicals) have been analyzed. The possibility that inactivation of these enzymes might accelerate senescence in cells that do not express telomerase has been assessed. Experiments have also been designed to determine whether treatment of cells with pro-oxidants such as iron and hydrogen peroxide accelerate senescence. Lastly, the role of chronic cell cycle arrest on the mechanism of senescence has been studied. Senescence of mutant cells containing inactivated cell

cycle checkpoint genes (*MEC2* and *RAD24*) was monitored and compared to normal cells. By exploring each of these potential regulators of *in vitro* cell aging, the results have made an important contribution to ongoing research in cellular aging and age-related diseases in humans.

CHAPTER 2

MATERIALS AND METHODS

I. MATERIALS

General reagents

Ammonium sulfate, sodium chloride and sodium dodecyl sulfate were purchased from Mallinckrodt AR (Paris, KY). Agarose and ethidium bromide were obtained from Sigma-Aldrich Chemical Co. (St. Louis, MO). Lithium acetate dehydrate, calcium chloride, 99% glycerol, polyethylene glycol (PEG-4000) and magnesium chloride were purchased from Sigma-Aldrich (St. Louis, MO). Sodium acetate was purchased from Mallinckrodt Baker, Inc. (Paris, KY). Tris base was purchased from Invitrogen Life Technologies (Carlsbad, CA). Hygromycin B (HygB) was purchased from Calbiochem-EMD Biosciences, Inc. (La Jolla, CA). G418 sulfate solution (G418) was purchased from Cellgro-Mediatech, Inc. (Herndon, VA). Nourseothricin-dihydrogen sulphate (Nat) was obtained from WERNER BioAgents (Meisenweg 7, Germany). 5-Fluoroorotic acid (5-FOA) was purchased from US Biological (Swampscott, MA).

Pro-oxidant reagents

Ferric chloride (FeCl_3) was manufactured by J.T. Baker Chemical Co. (Phillipsburg, NJ). Ferric ammonium sulfate ($\text{FeNH}_4(\text{SO}_4)_2$) was manufactured by Fisher Scientific Co. (Fair Lawn, NJ). Cadmium chloride, menadione sodium bisulfite and tert-butyl hydroperoxide (t-BHP) were purchased from Sigma-Aldrich (St. Louis, MO). Hydrogen peroxide (H_2O_2) was purchased from Calbiochem-EMD Biosciences, Inc. (La Jolla, CA).

Bacteriological and yeast growth media

All amino acids, D-(+)-glucose, and ampicillin were purchased from Sigma-Aldrich (St. Louis, MO). Bacto peptone, bacto yeast extract, bacto tryptone and bacto agar were obtained from Becton Dickinson Microbiological Systems (Sparks, MD). Galactose was purchased from Ferro Pfanstiehl Laboratories, Inc. (Waukegan, IL) and also from Sigma-Aldrich (St. Louis, MO).

Enzymes and PCR reagents

Restriction enzymes were purchased from New England Biolabs (Beverly, MA). Taq DNA polymerase, Vent DNA polymerase and Vent (exo⁻) DNA polymerase were purchased from New England Biolabs (Beverly, MA). Ex Taq DNA polymerase was obtained from Takara Mirus Bio (Madison, WI). T4 DNA Ligase and buffer were purchased from New England Biolabs (Beverly, MA).

Cell culture solutions and media

For general, nonselective growth, yeast cells were grown on YPGlu (YPDA; rich glucose) media (1% bacto yeast extract, 2% bacto peptone, 2% glucose, 2% bacto agar) or YPGal plates (1% bacto yeast extract, 2% bacto peptone, 2% galactose, 2% bacto agar). In order to assess mitochondrial function, yeast cells were grown on YPG media (1% bacto yeast extract, 2% bacto peptone, 3% glycerol, 2% bacto agar). For plasmid selection, yeast cells were grown on synthetic media with drop-out mix (2-3% glucose or 2% galactose, 2% bacto agar, plus all essential amino acids and bases except those used for plasmid selection). All quantities listed as “%” are w/v here and elsewhere. HygB and G418 antibiotic plates were prepared using YPGlu or YPGal media plus HygB or G418 mixed to 250 $\mu\text{g}/\text{mL}$ and 200 $\mu\text{g}/\text{mL}$ concentrations, respectively. Nourseothricin (Nat) antibiotic plates were prepared using YPGal media plus Nat mixed to 120 $\mu\text{g}/\text{mL}$ concentrations. Iron plates were prepared using rich or synthetic media plus FeCl_3 or $\text{FeNH}_4(\text{SO}_4)_2$ mixed to obtain various concentrations. Plates used to test H_2O_2 and t-butyl hydroperoxide sensitivity were prepared using synthetic or rich media plus H_2O_2 or t-butyl hydroperoxide mixed to obtain various concentrations. Menadione and cadmium plates were prepared similarly using synthetic media.

Yeast strains

The parent strains used for these studies were BY4742 (*MAT α his3 Δ 1 leu2 Δ 0 lys2 Δ 0 ura3 Δ 0*) and BY4741 (*MAT α his3 Δ 1 leu2 Δ 0 met15 Δ 0 ura3 Δ 0*). The *est2* strain utilized in initial assays was YLKL803 (BY4742, Δ *est2::HygB'* containing

plasmid pLKL82Y [*CEN/ARS URA3 GAL1-V10p::EST2*] (37). For testing oxidation sensitivity and senescence kinetics, genes encoding a glutathione peroxidase (Gpx3) or catalase enzyme (Ctt1) were inactivated. YLKL821 was created by inactivating the *GPX3* gene in strain YLKL803 to create a $\Delta gpx3::G418^r$ allele. The other oxidation mutant strain, YLKL820, was created by inactivating the *CTT1* gene in strain YLKL803 to create a $\Delta ctt1::G418^r$ allele. Two independently confirmed isolates were saved for each mutant. A double mutant, YLKL829, was created by inactivating the *GPX3* gene in strain YLKL820 to create a $\Delta gpx3::Nat1^r \Delta ctt1::G418^r$ strain. The lab also obtained BY4741 strain derivatives from Simon Avery at The University of Nottingham. The three strains were identified as: *yap1*-BY4741, *yap1 gpx3*-BY4741 and *gpx1 gpx2 gpx3*-BY4741. Once these strains were received, the isolates were streak purified and *EST2* was deleted as described below.

Yeast strains

All yeasts strains used in this study are listed in Table 1.

Table 1. *Saccharomyces cerevisiae* strains

Strain	Genotype	Reference/Source
BY4742	<i>MATα his3Δ1 leu2Δ0 lys2Δ0 ura3Δ0</i>	(32)
BY4741	<i>MATα his3Δ1 leu2Δ0 met15Δ0 ura3Δ0</i>	(32)
YLKL803	BY4742, Δ <i>est2</i> <i>HygB</i> ^r + pLKL82Y (<i>GAL1-V10::EST2, URA3</i>)	Lab strain
YLKL807	YLKL803, Δ <i>rad52</i> <i>G418</i> ^r	Lab strain
YLKL820	YLKL803, Δ <i>ctt1</i> <i>G418</i> ^r	This study
YLKL821	YLKL803, Δ <i>gpx3</i> <i>G418</i> ^r	This study
<i>yap1</i> -BY4741	BY4741, Δ <i>yap1</i> <i>G418</i> ^r	(33)
YLKL829	YLKL820, Δ <i>gpx3</i> <i>Nat</i> ^r	This study
<i>yap1 gpx3</i> -BY4741	BY4741, Δ <i>yap1</i> <i>G418</i> ^r Δ <i>gpx3</i> <i>URA3</i>	(33)
<i>gpx1 gpx2 gpx3</i> -BY4741	BY4741, Δ <i>gpx3</i> <i>G418</i> ^r Δ <i>gpx2</i> <i>HIS3</i> Δ <i>gpx1</i> <i>URA3</i>	(33)
YLKL833	YLKL803, Δ <i> mre11::G418</i> ^r	Lab strain
YLKL836	BY4741, Δ <i>est2</i> <i>HygB</i> ^r + pLKL82Y (<i>GAL1-V10::EST2, URA3</i>)	This study
YLKL837	YLKL836, Δ <i>yap1</i> <i>G418</i> ^r Δ <i>est2</i> <i>HygB</i> ^r + pLKL82Y (<i>GAL1-V10::EST2, URA3</i>)	This study
YLKL838	YLKL836, Δ <i>yap1</i> <i>G418</i> ^r Δ <i>gpx3</i> Δ <i>est2</i> <i>HygB</i> ^r + pLKL82Y (<i>GAL1-V10::EST2, URA3</i>)	This study
YLKL839	YLKL836, Δ <i>gpx3</i> <i>G418</i> ^r Δ <i>gpx2</i> <i>HIS3</i> Δ <i>gpx1</i> Δ <i>est2</i> <i>HygB</i> ^r + pLKL82Y (<i>GAL1-V10::EST2, URA3</i>)	This study
YLKL840	YLKL803, Δ <i>rad24</i> <i>G418</i> ^r	This study
YLKL841	YLKL803, Δ <i>mec3</i> <i>G418</i> ^r	This study
YLKL844	YLKL840, Δ <i>mec3</i> <i>Nat</i> ^r	This study

II. METHODS

Chromosomal and plasmid DNA purification

For chromosomal DNA, a MasterPure™ Purification Kit by Epicentre Technologies was used following the kit protocol. Several experiments required further chromosomal DNA purification using a Qiagen miniprep spin column purchased from QIAGEN, Inc. (Valencia, CA).

Yeast transformations

Yeast transformations were performed using either a high efficiency method described by Gietz *et al.* (34) or a rapid DMSO-based transformation method by Soni *et al.* (35).

Insertional inactivation of yeast genes

Gel electrophoresis was the technique used to confirm gene deletions in the yeast strains used in these experiments. Agarose gels were formed by mixing 0.7-0.8% agarose in aqueous 1X TBE (Tris-borate-EDTA) buffer. Approximately 5-6 µl of a prepared mix of DNA, TE buffer and loading dye was loaded per well. The loading dye was composed of a mix of glycerol, bromophenol blue and xylene cyanol.

Creation of *S. cerevisiae* strain YLKL821 lacking GPX3 ($\Delta est2::HygB'$

$\Delta gpx3::G418'$ –BY4742 mutants containing pLKL82Y)

PCR amplification of the G418' gene. The G418 resistance gene (*G418'*, also called Kan-MX) was amplified via PCR from the plasmid pFA6MX4 using primers gGPX3a (GAATTCTATAAGCTAGCACCTGTTGACAAGAAAGGCCAACCATTTCCCCTT) and gGPX3b (AGACCTGCCTATTCCACCTCTTTCAAAGTTCTTCGATGGTTTCGGACAA) and Ex Taq DNA polymerase. The reactions were exposed to the following conditions: 94° C for 2 minutes and then 34 cycles (94° C for 30 seconds, 42° C for 30 sec, 72° C for 1 min 45 sec) followed by extension of all unfinished strands at 72° C for 7 minutes. The PCR samples were analyzed by gel electrophoresis on a 0.8% agarose gel that was stained with ethidium bromide.

The *G418'* PCR fragment was transformed into strain YLKL803 via the high efficiency lithium acetate protocol (34). Transformants were spread to YPGlu plates and grown for 1 day at 30° C and then replica-plated to YPGal + G418 plates and incubated at 30° C for 2-3 days. Individual colonies were patch-purified onto YpGal + G418 plates and incubated at 30° C for 1-2 days. The patches were replica- plated to YPG and Glu-Ura. *GPX3* gene-deleted isolates were confirmed by their G418 resistance and by PCR.

Confirmation of GPX3 gene deletion. The *GPX3* gene deletions were confirmed by purifying genomic DNA from individual colonies and performing PCR

using test primers 5'GPX3 (ACCATGAGGAACAGTATGCTCC) and 3'GPX3 (TTGCGTTCGTACGGCACTAGCA) that anneal upstream and downstream of the *GPX3* gene coding sequence and Ex Taq polymerase. The reactions were exposed to the following conditions: 94° C for 2 minutes and then 32 cycles (94° C for 30 sec, 48° C for 30 sec, 72° C for 1 min 30 sec) followed by extension of all unfinished strands at 72° C for 7 minutes. The PCR samples were analyzed by gel electrophoresis on a 0.8% agarose gel.

Production of YLKL820 ($\Delta est2::HygB^r \Delta ct1::G418^r$ –BY4742 mutants containing pLKL82Y)

PCR amplification of the G418^r gene. The G418 resistance gene (*G418^r*) was amplified via PCR from the plasmid pFA6MX4 using primers gCTT1a (CTCATGCCAATAAGATCAATCAGCTCAGCTTCACAAATGAACGTGTTCCG) and gCTT1b (GTGCTGCCTTAATTGGCACTTGCAATGGACCAAGTCTTGGCATAACCTTC) and Ex Taq DNA polymerase. The reactions were exposed to the following conditions: 94° C for 2 minutes and then 34 cycles (94° C for 30 sec, 42° C for 30 sec, 72° C for 1 min 45 sec) followed by extension of all unfinished strands at 72° C for 7 minutes. The PCR samples were analyzed by gel electrophoresis on a 0.8% agarose gel.

The *G418^r* PCR fragment was transformed into strain YLKL803 via the high efficiency lithium acetate protocol. Transformants were grown on YPGlu at 30° C for 1 day and then replica-plated to YPGal + G418 and incubated at 30° C for 3 days.

Individual colonies were patch-purified onto YpGal + G418 and were incubated at 30° C for 2 days. The patches were replica plated to YPG and Glu-Ura. *CTT1* gene-deleted isolates were confirmed by their G418 resistance and by PCR.

Confirmation of CTT1 gene deletion. The *CTT1* gene deletion was confirmed by purifying genomic DNA from individual colonies and performing PCR using test primers 5'CTT1 (CACATTGTGCATTTATCGTATCCC) and 3'CTT1 (ACGACCAATTTGTAATAACTAGTG) and Ex Taq DNA polymerase. Reactions were as described above except an extension time of 1 min 30 sec was used.

Production of antioxidant gene double mutant strain YLKL829 ($\Delta est2::HygB^r$ $\Delta gpx3::G418^r$ $\Delta ctt1::Nat1^r$ -BY4742 mutants containing pLKL82Y)

The *Nat1* resistance gene was PCR amplified from the plasmid pAG25 using the primers gCTT1a and gCTT1b. Samples were run on a 0.8% agarose gel, stained with ethidium bromide and visualized. The resulting *ctt1::Nat1^r* fragments were pooled and used to transform strain YLKL821 (*$\Delta gpx3::G418^r$*). The mixture was spread and grown on YPGlu at 30° C for 2 days. The transformants were replica-plated to YPGlu, YPGal + Nat and Glu-Ura and incubated at 30° C for 2-3 days. Individual colonies were patch-purified onto YPGal + Nat, Glu-Ura and YPGlu + G418 and incubated at 30° C for 2 days. *CTT1* gene deleted isolates were confirmed by their *Nat1^r* resistance and by PCR using 5' CTT1 and 3'CTT1 test primers.

Production of YLKL836 ($\Delta est2::HygB'$ –BY4741 mutants containing pLKL82Y)

Phenotype Test to confirm Avery's published phenotypes characteristics.

Oxidation-sensitive strains $\Delta yap1::G418'$ -BY4741, $\Delta yap1::G418'$ $\Delta gpx3::URA3$ -BY4741 and $\Delta gpx3::G418'$ $\Delta gpx2::HIS3$ $\Delta gpx1::URA3$ -BY4741 were streaked onto YPGlu + G418 and incubated at 30° C for 2-3 days. Individual colonies were patched to YPGlu + G418 and later replica-plated to YPG, Glu-Ura, YPGlu + G418 and YPGlu-His and incubated at 30° C for 2-3 days. The phenotypes were consistent with the published descriptions provided by Simon Avery.

PCR amplification of the HygB' gene for deletion of EST2 in BY4741 and its derivatives. The Hygromycin B resistance gene (*HygB'*) was amplified via PCR from the pAG32 plasmid using primers gEST2a2 (CTCATGAAAATCTTATTCGAGTTCATTCAAGACAAGCTTGACATTGATCTACAGATGTGACTGTCGCCCGTACATT) and gEST2b2 (TCCTTATCAGCATCATAAGCTGTCAGTATTTTCATGTATTATTAGTACTAATTAACGACAAGTTCTTGAAAACAAGAATC) and Taq DNA polymerase enzyme. The reactions were exposed to the following conditions: 94° C for 2 minutes and then 34 cycles (94° C for 30 sec, 42° C for 30 sec, 72° C for 1 min 45 sec) followed by extension of all unfinished strands at 72° C for 7 minutes.

BY4741 was transformed with pLKL82Y (*GAL1-V10p::EST2 CEN/ARS URA3*) to produce Ura⁺ colonies that could express *EST2* from the plasmid. The $\Delta est2::HygB'$ PCR fragment was transformed into BY4741 (with pLKL82Y) cells via the high efficiency protocol. Transformants were grown on YPGlu at 30° C for 1 day

and then replica-plated onto YPGal + HygB and incubated at 30° C for 3 days.

Individual colonies were patch-purified onto YpGal + HygB, Glu-Ura and YPG and incubated at 30° C for 1-2 days.

Confirmation of EST2 gene deletion. The *EST2* gene deletion was confirmed by purifying genomic DNA from individual colonies and performing a PCR using test primers 5'EST2b (GAGCTATTGGTGATTCGCATTTAGGA) and 3'EST2b (GGGAGGCTTTGAAGAAGTAGAAAGGA) and Ex Taq DNA polymerase. The reactions were exposed to the following conditions: 94° C for 2 minutes and then 32 cycles (95° C for 20 sec, 38° C for 40 sec, 72° C for 2 min) followed by extension of all unfinished strands at 72° C for 7 minutes.

Production of YLKL837 ($\Delta yap1::G418^r \Delta est2::HygB^r$ -BY4741 mutants containing pLKL82Y)

PCR amplification of the HygB^r gene. The Hygromycin B resistance gene (*HygB^r*) was amplified via PCR from the pAG32 plasmid using gEST2a2 and gEST2b2 primers and Taq polymerase as described above.

yap1-BY4741 cells were transformed with pLKL82Y (*GAL1-V10p::EST2 CEN/ARS URA3*) to produce Ura⁺ colonies that could express *EST2* from the plasmid. The *Δest2::HygB^r* PCR fragment was transformed into YLKL826 via the high efficiency protocol and grown as described previously. *EST2* gene-deleted isolates were confirmed by their HygB resistance and by PCR using 5'EST2b and 3'EST2b test primers.

Confirmation of EST2 gene deletion. The *EST2* gene deletion was confirmed by purifying genomic DNA from individual colonies and doing a PCR using 5'EST2b and 3'EST2b test primers and Ex Taq DNA polymerase. The reactions were exposed to the following conditions: 94° C for 2 minutes and then 32 cycles (95° C for 20 sec, 38° C for 40 sec, 72° C for 2 min) followed by extension of all unfinished strands at 72° C for 7 minutes.

Production of YLKL838 ($\Delta yap1::G418^r \Delta gpx3::URA3 \Delta est2::HygB^r$ -BY4741 mutants containing pLKL82Y)

To create a *ura3⁻* derivative, *$\Delta yap1::G418^r \Delta gpx3::URA3$* cells were spread to synthetic plates containing 0.2 mg/ml 5-FOA (5-fluoroorotic acid). This drug is toxic to *URA3⁺* cells so that only spontaneously occurring *ura3⁻* mutants are able to form colonies. Two independent isolates that were stable (non-reverting) were identified that did not form revertant colonies even when $\geq 10^7$ cells were later spread onto a Glu-Ura plate. This new *ura3⁻* derivative was called YLKL830.

PCR amplification of the HygB^r gene. The Hygromycin B resistance gene (*HygB^r*) was amplified as before using gEST2a2 and gEST2b2 primers and Taq polymerase. Cells of the new strain YLKL830, *$\Delta yap1::G418^r \Delta gpx3$* -BY4741 were transformed with pLKL82Y (*GAL1-V10p::EST2 CEN/ARS URA3*) to produce Ura⁺ colonies that could express *EST2* from the plasmid. The *$\Delta est2::HygB^r$* PCR fragment was then transformed into these plasmid-containing cells via the high efficiency protocol. Transformants were grown on YPGlu and individual colonies patch-

purified as before. *EST2* gene-deleted isolates were confirmed by their HygB resistance and by PCR using 5'EST2b and 3'EST2b test primers and the new strain was designated YLKL838.

Production of YLKL839 ($\Delta gpx3::G418^r$ $\Delta gpx2::HIS3$ $\Delta gpx1 \Delta est2::HygB^r$ -BY4741 mutants containing pLKL82Y)

$\Delta gpx1::URA3$ $\Delta gpx2::HIS3$ $\Delta gpx3::G418^r$ -BY4741 cells were spread to synthetic 5-FOA plates, which selects against *URA*⁺ (plasmid containing) cells, as before. Individual colonies were streak-purified onto fresh 5-FOA plates. Several individual colonies were selected and spread to Glu-Ura to confirm that they were non-reverting. The new *ura3*⁻ derivative was designated YLKL831.

PCR amplification of the HygB^r gene. The Hygromycin B resistance gene (*HygB^r*) was amplified via PCR from the plasmid pAG32 using gEST2a2 and gEST2b2 primers and Taq polymerase as mentioned before.

Cells of the new strain YLKL831 were transformed with pLKL82Y (*GALI-V10p::EST2 CEN/ARS URA3*) to produce Ura⁺ colonies that could express *EST2* from the plasmid. The *$\Delta est2::HygB^r$* PCR fragment was then transformed into these plasmid-containing cells via the high efficiency protocol and grown as previously described. *EST2* gene-deleted isolates were confirmed by their HygB resistance and PCR using 5'EST2b and 3'EST2b test primers. The new strain was designated YLKL839.

Production of checkpoint defective strain YLKL840 ($\Delta est2::HygB'$ $\Delta rad24::G418'$) containing pLKL82Y

PCR amplification of the G418' gene. The G418 resistance gene (*G418'*) was amplified via PCR from plasmid pFA6MX4 using primers gRAD24a (AGTTAGAGTATTTCCAGATCTGAATCTGAAAGGGACTCACTGATAACTGGGACAAGTTCTTGAAAACAAGAATC) and gRAD24b (AGTTAGAGTATTTCCAGATCTGAATCTGAAAGGGACTCACTGATAACTGGGACAAGTTCTTGAAAACAAGAATC) and Taq polymerase.

The *G418'* PCR fragment was transformed into YLKL803 and transformants were grown on YPGlu at 30° C for 2 days and then replica-plated to YPGal + G418 and incubated at 30° C for 2-3 days. Individual colonies were patch-purified onto YpGal + G418, Glu-Ura and YPGlu + HygB and incubated at 30° C for 1 day. *RAD24* gene-deleted isolates were confirmed by their G418 resistance and by PCR.

Confirmation of RAD24 gene deletion. The *RAD24* gene deletion was confirmed by purifying genomic DNA from individual colonies and performing PCR using test primers 5'*RAD24*(#2) (GATATCTGAGAGATCATCACAATGCGT) and 3'*RAD24*(#2) (GAATGTAATGTGCATAGATTTGTGTGGA) and Ex Taq DNA polymerase as described.

Production of checkpoint mutant strain YLKL841 ($\Delta est2::HygB^r \Delta mec3::G418^r$) containing pLKL82Y

PCR amplification of the G418^r gene. The G418^r gene was amplified via PCR from plasmid pFA6MX4 using primers gMEC3a (CAGTTAAATGAAATTTAAAATTGATAGTAAATGGTTGTGAAGCACCTGATGATGTGACTGTGCGCCCGTACATT) and gMEC3b (TTAGCAACGTAGCAAAGAAATGTACCGCTGTAGGGTTTACAAGCCCTTCGGACAAGTTCTTGAAAACAAGAATC) and Vent (exo⁻) enzyme. The reactions were performed essentially as described previously.

The G418^r PCR fragment was transformed into YLKL803 and transformants were grown as before. MEC3 gene-deleted isolates were confirmed by their G418 resistance and by PCR.

Confirmation of MEC3 gene deletion. The MEC3 gene deletion was confirmed by purifying genomic DNA from individual colonies and performing a PCR using test primers 5' MEC3(#2) (AAGGTGTGTCTTAATTCAGTTAAATGAA) and 3' MEC3(#2) (CTGCAGTTCTCAGCCATGTCAGATT).

Production of the checkpoint double mutant strain YLKL844 ($\Delta est2::HygB^r \Delta rad24::G418^r \Delta mec3::Nat1^r$) containing pLKL82Y

The Nat1 resistance gene (*Nat1^r*) was PCR amplified from plasmid pAG25 using the gMEC3a and gMEC3b primers and Taq DNA polymerase. Samples were

run on a 0.8% agarose gel, stained with ethidium bromide and visualized. The *NatI^r* gene fragment was then transformed into $\Delta est2::HygB^r \Delta rad24::G418^r$ -BY4742 cells containing pLKL82Y (strain YLKL840). Transformants were spread to YPGlu and incubated for 2 days at 30° C. Plates containing the transformants were replica-plated to YPGal + Nat and incubated at 30° C for 2 days. Transformants were replica-plated to YPGlu + HygB, Glu-Ura and YPGlu + G418 and incubated at 30° C for 2 days. Individual colonies from original transformants on YPGal + Nat plates were patch-purified onto YPGal + Nat, YPGlu + G418 and Gal-Ura plates and grown for 2-3 days at 30° C. *MEC3* gene-deleted isolates that were *Nat^r*, *G418^r* and *URA3⁺* were then tested by PCR using 5' *MEC3* (#2) and 3' *MEC3* (#2) primers to confirm the deletion.

Solid media-based senescence assays

Cell senescence was observed by streaking telomerase-deficient and wildtype control cells from the low density regions of a freshly streaked Gal-Ura stock plate using sterile toothpicks onto YPGlu (rich) or synthetic Glu-Ura plates. These cells were grown for 2 days (YPGlu) or 3 days (synthetic Glu-Ura) at ~23° C, 30° C, 37° C or 40° C. After the first streak, cells were re-streaked from moderate-sized individual colonies onto a fresh YPGlu or Glu-Ura plate again and the process was repeated until senescence occurred. The senescing cells were defined by their loss of the ability to grow compared to the wildtype control cells that would grow indefinitely. The apparent senescent phenotype was visible by the fourth streak in

BY4742 cells and the fifth streak in BY4741 strains (~60-80 generations). Images of each streak were captured using a Canon powershot G3 digital camera and saving images as .jpg formatted files. The senescence assay was followed to test cellular senescence in all the mutant strains developed in this project.

UV sensitivity test

The UV sensitivity of wildtype and checkpoint-deficient cells was tested by streaking them onto YPGlu or YPGal plates and growing at 30° C for 2-3 days. These cells were then replica-plated to a fresh YPGlu plate and exposed to ultra violet light for various time lengths and incubated for 2-3 days at 30° C. The source of UV was provided by a transilluminator purchased from FOTODYNE, Inc.

Cell-cycle stage quantitation

Strains lacking a checkpoint protein (Mec3 or Rad24) fail to arrest in the G₂ phase of the cell cycle in response to DNA damage. Checkpoint deficient cells die as a result of increased levels of DNA damage that are not repaired because the cells do not pause in the cell cycle to allow time for repair. To assess the effects of checkpoint-deficient cells and senescence, cell cycle counts were performed. Cells undergoing senescence increase significantly in size and most cells activate cell cycle checkpoints in response to the shortened telomeres which may appear as broken ends. Senescent cells eventually arrest permanently with most cells forming large-budded (G₂) cells. Aliquots were taken from liquid cultures and were diluted,

sonicated, and loaded onto a hemacytometer. The cell types were analyzed using a phase contrast microscope (LOMO Comcon Microscope). Cell cycle stage was quantitated as follows: unbudded cells were classified as being in G₁ phase, cells with small buds attached were in S phase and cells with large buds were in G₂/M (primarily G₂ phase) (36).

EST2 reactivation and senescent cell holding assays

Initial *EST2* reactivation studies were done by streaking *est2*⁻-BY4742 cells containing the *GAL1-V10::EST2* fusion plasmid (YLKL803) from a fresh Gal-Ura plate to a Glu-Ura plate. Cells were grown for three days at 30° C before restreaking onto a fresh Glu-Ura plate and grown for 3 more days. The next streak (third streak) was allowed to grow four days, as was the fourth streak. From the third streak, colonies were harvested, diluted, sonicated and counted using a hemacytometer. Fourth streak colonies were also harvested and counted. Cells were spread to galactose and glucose plates to determine whether late senescent cells could be rescued by reactivation of telomerase expression. The colony forming ability of cells was tested by measuring the plating efficiency, which is defined as the number of cells able to form colonies on plates divided by the number of cells in the culture counted microscopically.

Later, reactivation experiments involving checkpoint single and double mutants were tested to compare their survival rates to those of checkpoint-proficient strains. In this experiment, two isolates of the single checkpoint mutants (*ctt1*⁻ or *gpx3*⁻), the

double checkpoint mutant, *est2⁻* control mutants and wildtype cells were streaked onto Glu-Ura for the first streak. After the third streak, seven colonies of each mutant were harvested, sonicated, counted, diluted and spread to galactose and glucose plates to determine whether late senescent cells lacking either or both essential checkpoint genes could be rescued efficiently by reactivation of telomerase expression.

Lastly, for the holding experiments, *est2⁻* -BY4742 cells were streaked onto Glu-Ura for the first and second streaks as before. After cells had undergone ~ 40 generations in the two streaks, colonies were harvested and counted as mentioned previously. Volumes were calculated to spread cells for the third plate, instead of streaking to get well-separated colonies. The cells grew for three days before harvesting seven colonies and spreading to both galactose and glucose plates to monitor the rates of reactivation. The original third growth plate (similar to a third streak) was placed back into the 30°C incubator and left for two more days. Seven colonies were harvested again, counted and spread to galactose and glucose plates as done prior for the third spread. The original third plate was placed back into the 30°C incubator again and the same process of harvesting, counting and spreading to galactose and glucose plates was repeated three more times. Ultimately, the third growth plate was held in the incubator for twelve consecutive days creating the name “holding experiment” for the assay.

CHAPTER 3

RESULTS AND DISCUSSION

The focus of this research project involves assessing nutritional and environmental parameters that influence the rate of cell senescence *in vitro*. Senescence occurs when the ends of chromosomes, the telomeres, have progressively shortened, which ultimately leads to cell death. Telomeres are specialized structures that serve to protect the ends of chromosomes from degradation and other DNA damage. When cells lack telomerase, an end-specific RNA-dependent DNA polymerase, the telomeres will progressively shorten with every phase of DNA replication. The telomerase complex consists of several protein subunits and an RNA template. The subunit of primary interest in this project was the Est2 polymerase particularly because the lab created a regulatable *EST2* expression system that enabled modulation of *in vitro* cell aging. The *EST2* expression system was created by transforming BY4742 yeast cells with a plasmid, pLKL82Y, which contains the Est2 polymerase (*EST2*) of telomerase under the control of a modified galactose-inducible *GAL1* promoter, called *GAL1-V10*. The promoter has reduced basal expression when cells are grown in glucose media. On the other hand, the promoter is strongly induced when cells are grown in galactose media. As shown in Figure 3, when yeast cells are grown on plates containing galactose, *EST2* is expressed from the pLKL82Y plasmid and cells grow as normal. When cells are grown

on glucose media, they do not express *EST2*, telomeres shorten every cell cycle and therefore the cells senesce after approximately 60-80 generations. This new system allows one to characterize senescence in detail.

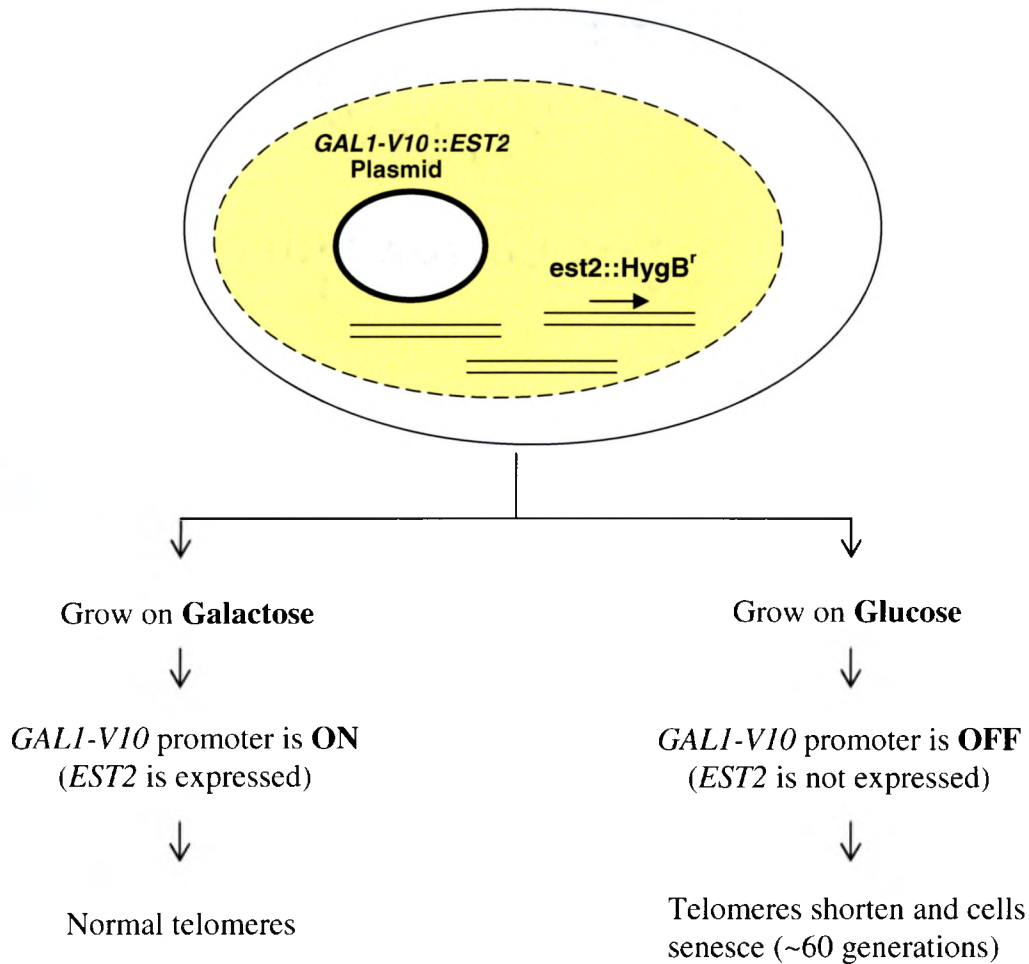


Figure 3. The system created to modulate *EST2* expression and cellular senescence in yeast.

In order to fully understand cellular senescence, the parameters that affect the rate of senescence need to be addressed. In this project, senescence could be detected as a reduced ability to form colonies and a change in colony size when streaked onto solid

media. Several isolates (usually 2-6) were streaked onto each plate to provide statistical confidence with the data and senescence. When streaked on plates, yeast cells divide approximately twenty times forming colonies (Figure 4). However, telomerase-deficient BY4742 cells consistently stop growing by the 4th streak, when telomere shortening has reached a critically shortened level. The senescence phenotype is observed on both rich (YPGlu) and synthetic (defined) media as demonstrated below on the fourth streak with telomerase-deficient cells. Cells grow faster on rich media, so YPGlu streaks were performed every 2 days while synthetic glucose plates were streaked every 3 days. Several parameters (e.g., caloric restriction, growth temperature and levels of oxidation) were tested by monitoring their effect on the rate of senescence using the streak assay.

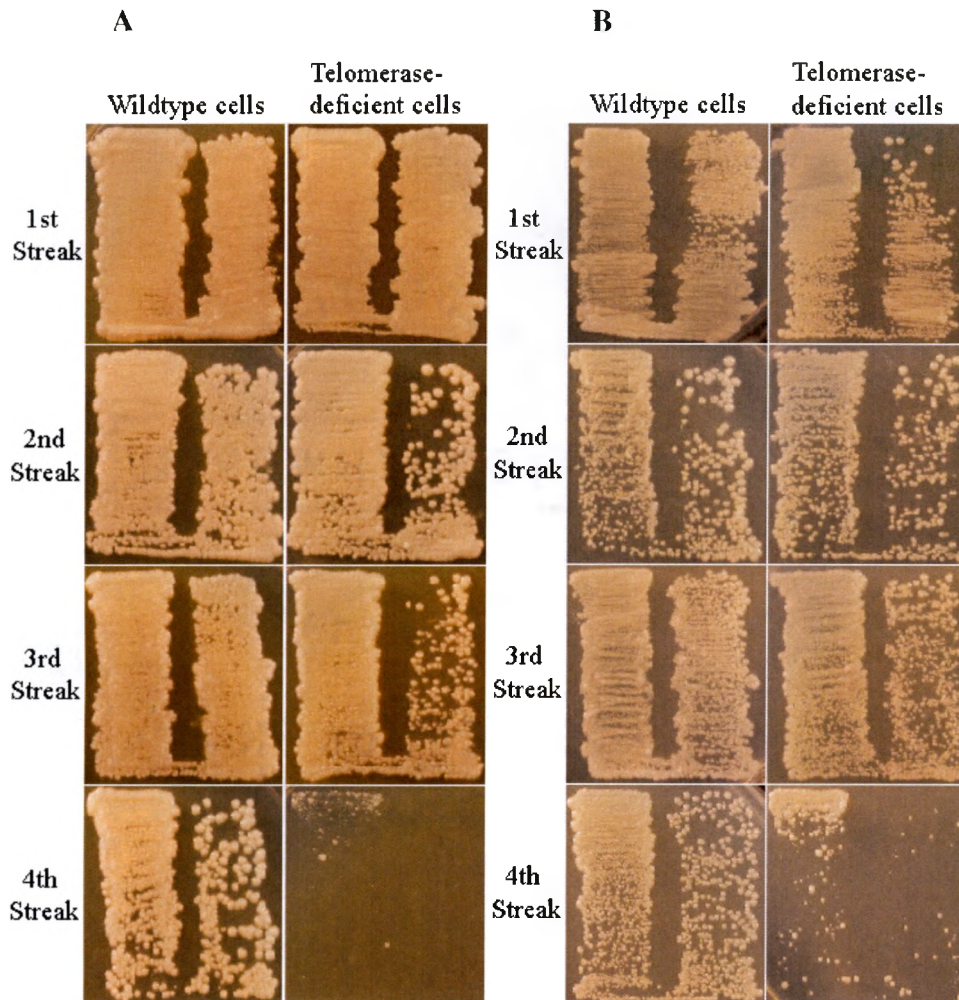


Figure 4. Wildtype BY4742 cells and mutant *est2⁻* cells that contain the *GALI-VI0p::EST2* fusion grown on (A) YPGlu (rich) or (B) synthetic (defined media) glucose plates. The mutant cells exhibit senescence on the 4th streak.

Initially, experiments were conducted to learn more about the effects of varying sugar concentrations and temperatures of incubation on telomerase-deficient cells used in the senescence streak assay. In many organisms, from yeast to mammals, evidence suggests that by restricting caloric intake, lifespan can be increased (11). The question

that needed to be addressed was whether increasing or decreasing the standard concentration of glucose (restricting cells of carbohydrates) in culture would affect the rate of senescence. The concentrations that were tested in this experiment, from lowest to highest, were 0.02%, 0.1%, 0.5%, the standard 2.0-3.0% and 8.0% glucose. Yeast cells were streaked onto plates containing the various glucose concentrations and were incubated at 30° C (Figure 5). The normal BY4742 cells (telomerase-proficient) were streaked every three days and could grow indefinitely at every concentration (data not shown).

Telomerase-deficient cells were streaked every three days and incubated at 30° C. Streak one and two are not shown due to their similarity. Telomerase-deficient cells on 8% glucose (the highest concentration) appeared to undergo fewer generations than cells grown on 3 % glucose (note the reduced growth on the 4th streak). The high glucose concentration effects might result from changes in osmotic pressure within the cell membranes. Due to a high influx of glucose, cells could have had difficulty adapting to the hypertonic environment and this additional stress may have accelerated the loss of viability. The 0.1% and 0.5% glucose concentrations did not have any impact on senescence. However, after a one hundred fold decrease from the standard amount to 0.02% glucose, fewer survivor mutants (seen as very large colonies) were observed when compared to cells streaked onto 2.0% glucose and colony sizes were only slightly smaller than those of cells grown in normal glucose. Survivor mutants are rare cells that have acquired a mutation that causes cellular levels of homologous recombination between telomeres to increase, thereby stabilizing them (26). In the senescence streak assay, the survivor mutants are identified as enlarged colonies usually seen in the fourth streak. We

have not quantitated this effect, but have simply noted a consistent difference in the number of enlarged survivor mutant colonies.

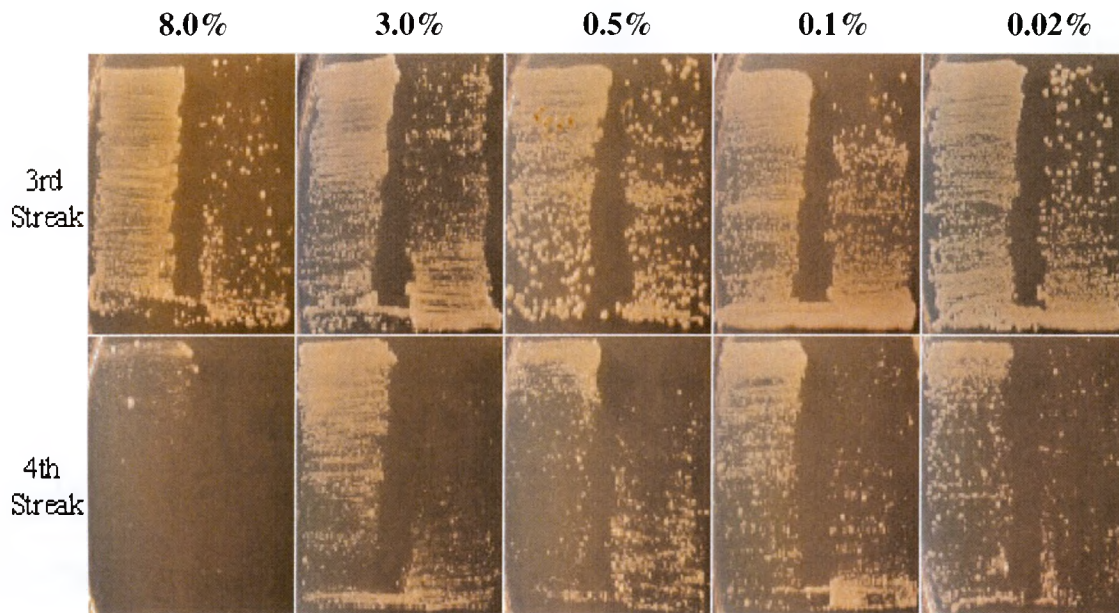


Figure 5. Mutant *est2⁻* cells streaked onto various plates containing 8.0%, 3.0%, 0.5%, 0.1% or 0.02% glucose.

In addition to variations in sugar concentration, incubation temperatures were also varied to determine whether an increase or decrease in growth temperature would affect the rate of senescence in telomerase-deficient cells. Studies have shown that above-optimum growth temperature induces internal stress within cells activating physiological responses. The optimum growth temperature for yeast is 30°C compared to *E. coli* and human cells' optimum temperature of 37°C. Yeast cells were initially grown at three different temperatures, 25°C, 30°C and 37°C by streaking cells onto 3% glucose plates. Cells were restreaked from individual colonies every three days (Figure 6). Due to a slower growth rate of cells at ~25° C, cells were incubated for four days after each streak.

There was an advantage of incubating yeasts at lower than normal temperatures and that is an apparent reduced level of survivor mutants. The assays also revealed that cells streaked onto 3% glucose and incubated at 37° C consistently had less growth on the fourth streak than cells grown at the normal 30° C incubation temperature.

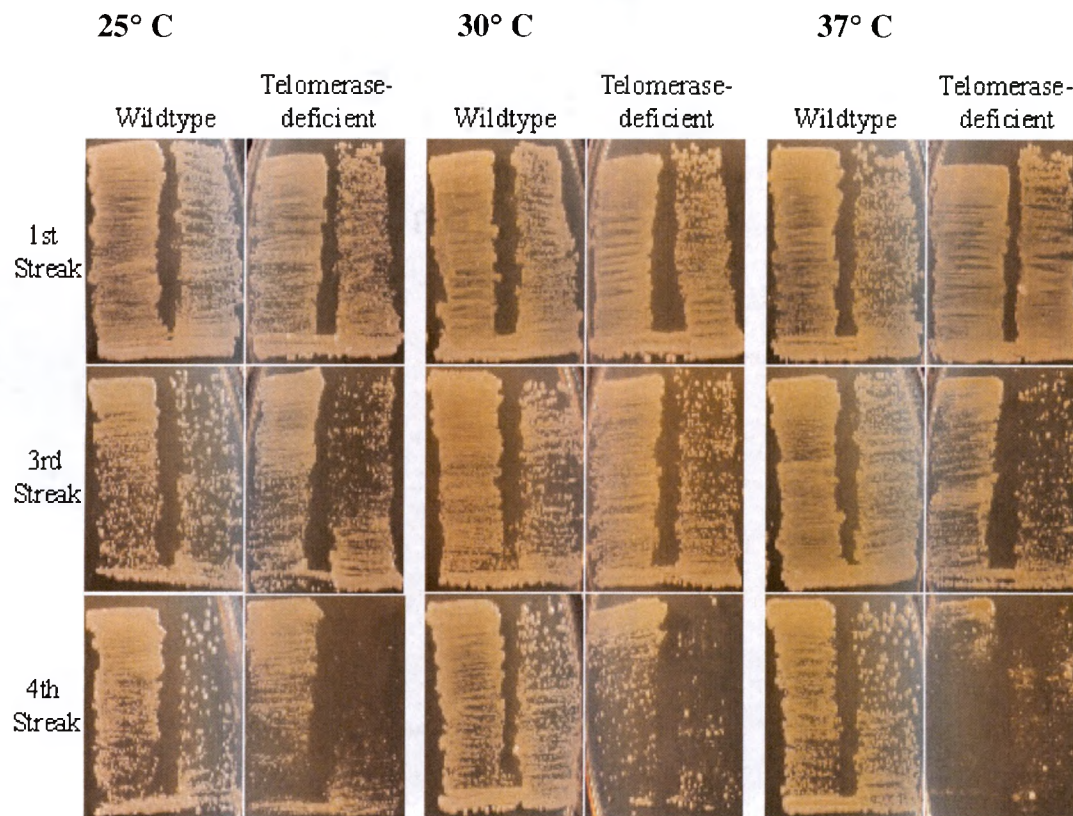


Figure 6. Growth of wildtype BY4742 and mutant *est2* cells at 25°, 30° and 37° C.

High temperatures have been associated with elevating a physiological response that activates a heat shock response. Heat shock proteins are expressed and help prevent proteins from heat denaturation by stabilizing proper protein structure and shape. Proteases are also induced that degrade irreversibly unfolded proteins. This heat shock

response helps organisms survive high temperature environments. In another temperature variation experiment, growth of cells on rich (YPGlu) or synthetic glucose media at 40°C and 30°C was tested (Figure 7). A stronger and cleaner senescent phenotype was observed at 40°C compared to 30°C. The cause of the enhanced senescence (fewer surviving colonies on the fourth streak) at high temperature is unclear.

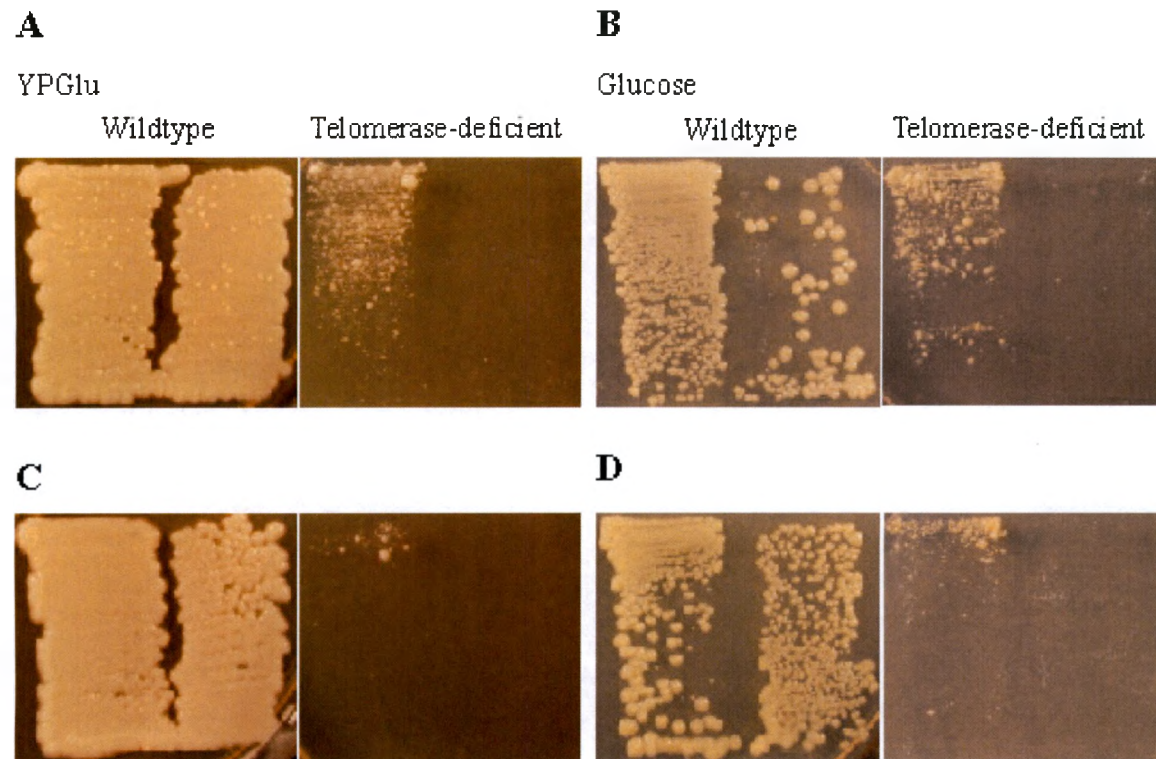


Figure 7. Mutant *est2⁻* cells were streaked onto (A) YPGlu for the 4th streak at 30°C or (B) synthetic plates at 30°C. (C) Cells streaked onto YPGlu and incubated at 40°C. (D) Cells streaked onto synthetic plates at 40°C.

Caloric restriction did not alter the rate of senescence and elevated growth temperature had only modest effects. The focus of this project turned to investigate the role of oxidation on *in vitro* cell aging. Oxidative damage can be induced in DNA and other macromolecules by a variety of reactive oxygen species (ROS). A consequence of

exposure to ROS is that cells accumulate damage to chromosomal DNA. Previous work has suggested that increased levels of oxidation are associated with accelerated senescence of human fibroblast cells *in vitro* and possibly *in vivo* (16).

Preliminary analysis of the impact of well-characterized pro-oxidants on *in vitro* cell aging

Using the regulatable *EST2* expression system, the role of oxidative DNA damage in senescing cells was assessed. The effects of oxidation on the rate of senescence were monitored by streaking yeast cells onto plates containing one of the following pro-oxidants: iron, hydrogen peroxide (H_2O_2), tert-butyl hydroperoxide (t-BHP), menadione or cadmium chloride.

The effects of various concentrations of iron, in the form of FeCl_3 or $\text{FeNH}_4(\text{SO}_4)_2$, on senescence was monitored by using the senescence streak assay. Iron is known to promote oxidation of biomolecules, especially via Fenton reactions (38). A high concentration of either FeCl_3 or $\text{FeNH}_4(\text{SO}_4)_2$ was toxic and lethal for both wildtype and telomerase-deficient cells. At 10 mM FeCl_3 and 5 mM $\text{FeNH}_4(\text{SO}_4)_2$ cells could not grow to form colonies. At slightly lower concentrations, telomerase-deficient cells grew and senesced normally on the fourth streak at 3 mM FeCl_3 and at 2 mM $\text{FeNH}_4(\text{SO}_4)_2$ (Figure 8-A and data not shown). Thus, iron did not have a significant influence on the rate of senescence.

Hydrogen peroxide is a powerful oxidizer that generates hydroxyl radicals in the presence of metal ions (referred to as the Fenton reaction) that cause damage to biomolecules within cells. In these experiments, glucose plates were prepared with

several concentrations of H_2O_2 to maximize the best conditions for observing senescence. Cells were incubated at 30°C and restreaked every three days. As shown in Figure 8, telomerase-deficient cells undergo senescence in the presence of $0.5\text{ mM H}_2\text{O}_2$ after four streaks. Other concentrations were examined but did not show a phenotype any different from that on $0.5\text{ mM H}_2\text{O}_2$. After several tests, it was concluded that H_2O_2 alone did not have any significant effects on cell senescence in *S. cerevisiae*.

Results from the two previous experiments testing pro-oxidants iron and H_2O_2 led to another question and experiment. Iron and H_2O_2 alone did not affect senescence; however, the rate of telomere shortening might be more greatly affected in the presence of both pro-oxidants because of increased cellular levels of oxidation. Control plates with 3 mM FeCl_3 and $0.5\text{ mM H}_2\text{O}_2$ alone were streaked every 3 days and incubated at 30°C (Figure 8-A and C). A third streak assay was conducted to test the rate of senescence in telomerase-deficient cells in the presence of both iron and H_2O_2 (Figure 8-B). Although colony size on the 3rd streak were smaller than controls, the combination of iron and H_2O_2 did not have any considerable effects on the kinetics of senescence (i.e., similar senescence was observed on streak 4 on all plates).

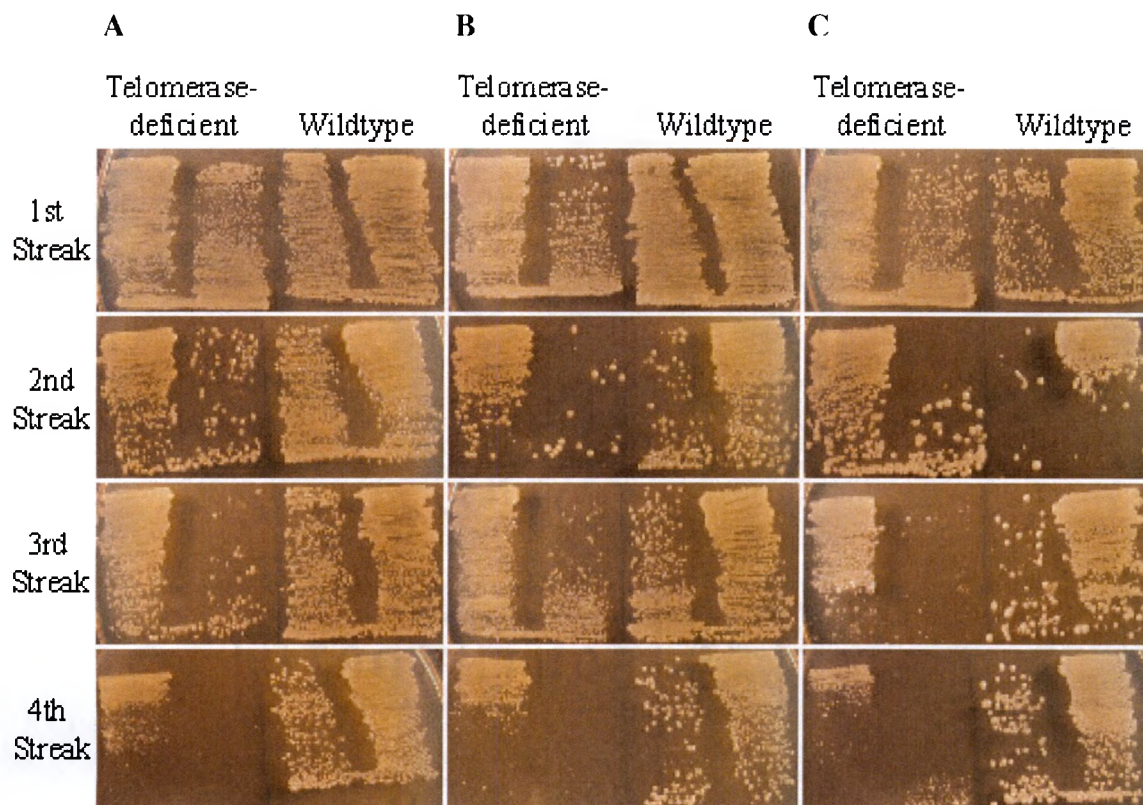


Figure 8. Growth of wildtype BY4742 and mutant *est2⁻* cells in the presence of (A) 3 mM FeCl₃ (B) 0.5 mM H₂O₂ + 3 mM FeCl₃ and (C) 0.5 mM H₂O₂.

Another pro-oxidant, tert-butyl hydroperoxide (t-BHP) was also investigated. t-BHP has been shown to increase intracellular levels of ROS (39). Cells were exposed to 0.25 mM, 0.5 mM and 0.75 mM t-BHP to determine whether increased levels of ROS would affect the rate of senescence. Wildtype and telomerase-deficient cells were streaked onto synthetic media with the various concentrations of t-BHP and incubated at 30°C. Telomerase-deficient cells grown on 0.25 mM t-BHP senesced in the normal four streaks (Figure 9-A). When the concentration was increased to 0.5 mM or 0.75 mM t-BHP, growth of the cells, especially with wildtype cells, was seriously compromised (Figure 9-B and C). The experiment was repeated and the results confirmed the previous

0.5 mM and 0.75 mM t-BHP observations. The effects of t-butyl hydroperoxide on wildtype BY4742 cells are currently under evaluation to understand the mechanism that is affecting wildtype more than telomerase-deficient cells.

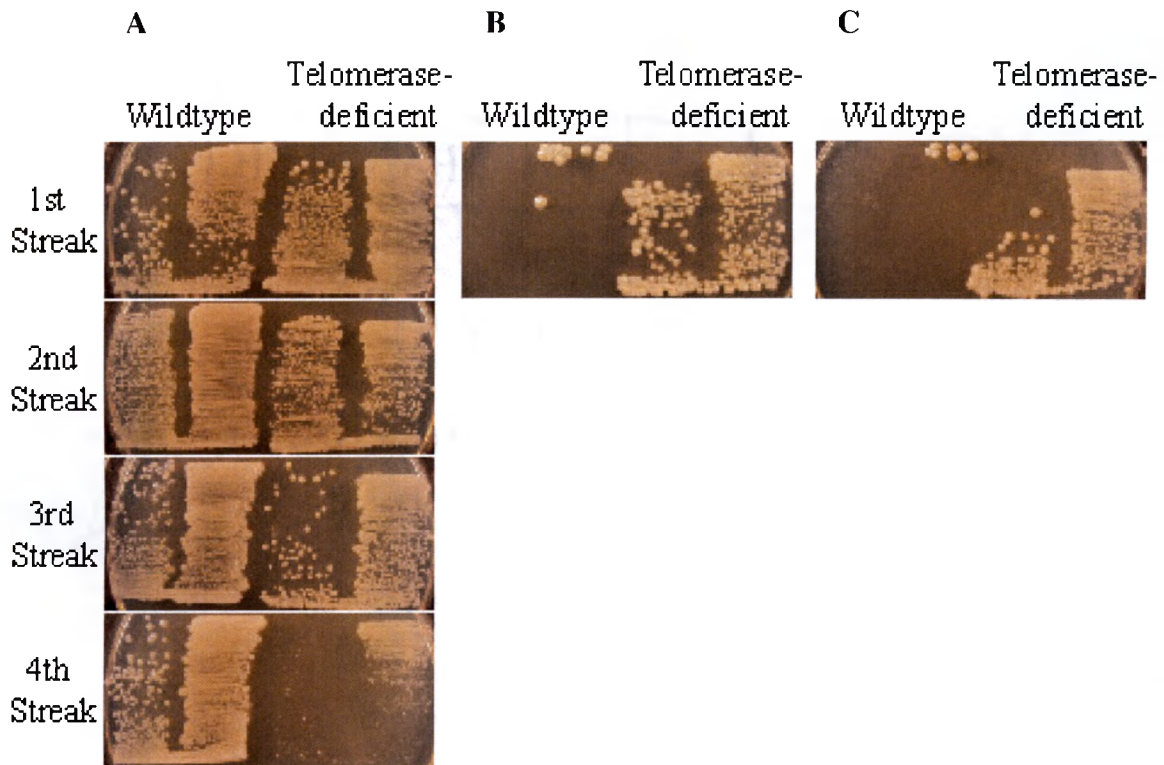


Figure 9. Wildtype BY4742 and *est2*⁻ cells streaked on glucose plates containing (A) 0.25 mM t-BHP (B) 0.5 mM t-BHP or (C) 0.75 mM t-BHP.

In another experiment, menadione (a source of superoxide radicals) was added to yeast cells to investigate its influence on senescence. Menadione has been shown to increase levels of oxidative damage when added to cells (40). In this experiment, 0.025 mM and 0.1 mM menadione was added to synthetic plate media to test whether telomerase-deficient cells were sensitive and would senesce at a different rate. The higher concentration of menadione exerted toxicity. The high dose demonstrated a

growth inhibition effect such that neither strain could grow normally after the 1st streak (Figure 10-B). When cells were streaked at the lower 0.025 mM menadione concentration, telomerase-deficient cells senesced normally on the fourth streak (Figure 10-A).

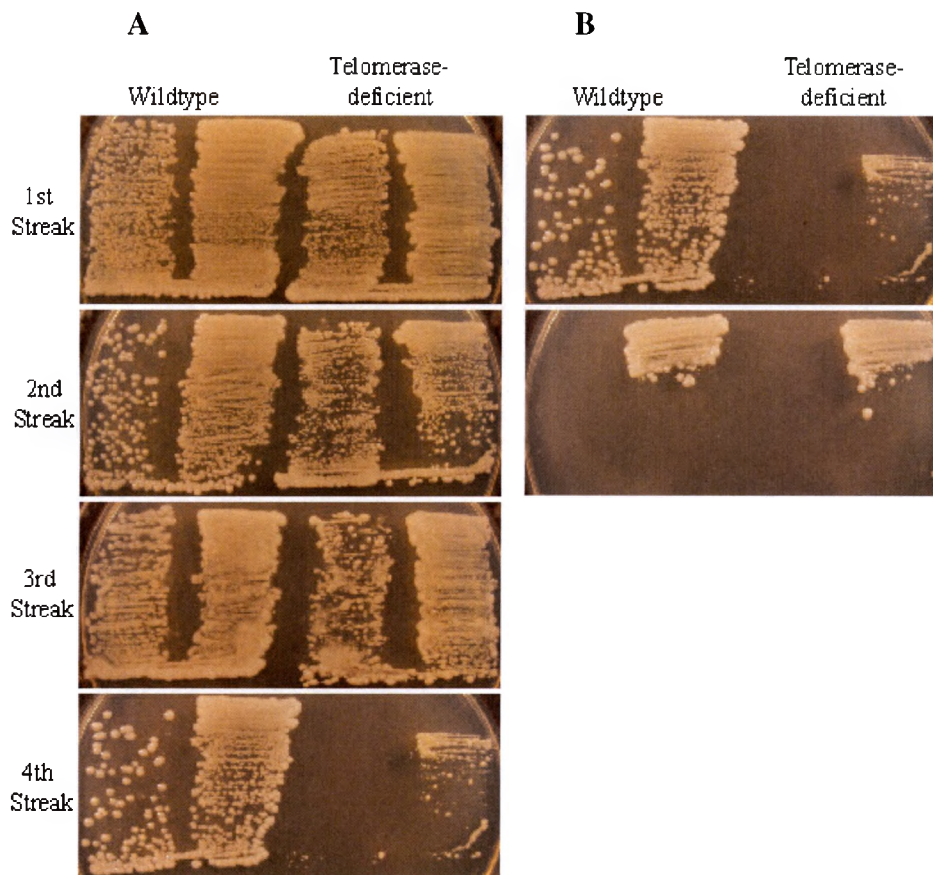


Figure 10. Wildtype BY4742 and mutant *est2⁻* cells were streaked onto glucose plates containing (A) 0.025 mM menadione or (B) 0.1 mM menadione.

The last pro-oxidant chemical tested in these studies was cadmium. Cadmium is a carcinogen that induces oxidative stress in cells via multiple mechanisms (17). In this experiment, two concentrations of cadmium, 0.025 mM and 0.1 mM, were used to determine whether cadmium influences the rate of telomere shortening. As shown in

Figure 11-B, 0.1 mM CdCl₂ inhibited growth of both wildtype and *est2*⁻ cells. The lower sublethal dose permitted growth, but did not alter the rate of *est2*⁻ cell senescence.

Interestingly, wildtype (BY4742) cells displayed an increased fraction of very large colonies amidst many smaller colonies on the 2nd, 3rd and 4th streaks (Figure 11-A). It is likely that the Cd²⁺ has stimulated a high rate of DNA mutation in the cells, resulting in an increased fraction with elevated cadmium-resistance. The results in Figure 11 indicated that senescence was not accelerated by the addition of cadmium.

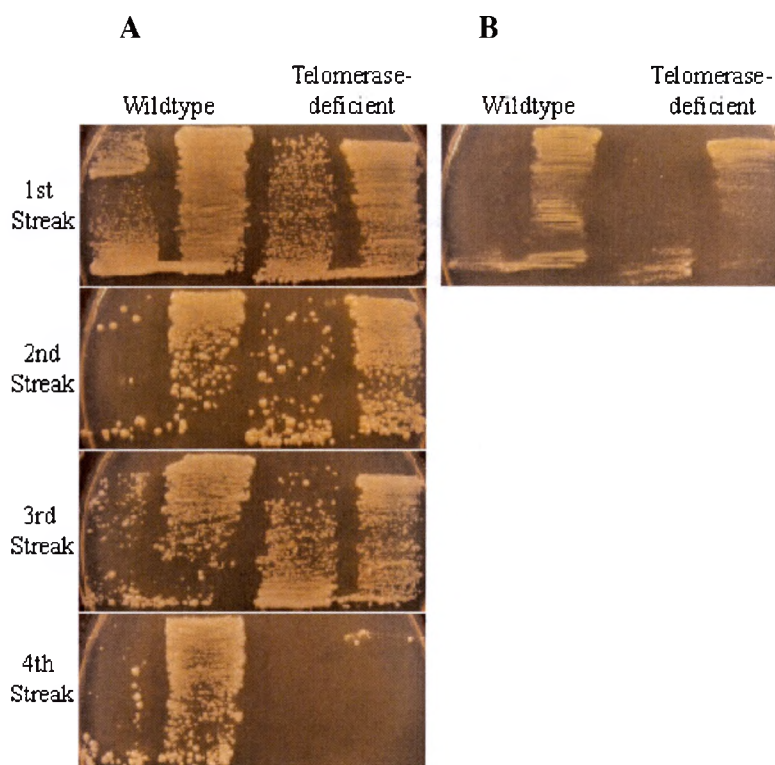


Figure 11. Wildtype BY4742 and mutant *est2*⁻ cells streaked onto (A) 0.025 mM cadmium or (B) 0.1 mM cadmium.

Inactivation of genes involved in resistance to oxidative damage and their effects on the rate of senescence

The next phase of the project required inactivation of genes involved in cell resistance to oxidative DNA damage to observe their effect on the rate of senescence. Previous studies have indicated that inactivation of certain DNA repair genes involved in double-strand break repair can modestly accelerate senescence in liquid culture assays. Such genes include *RAD52* and *MRE11* (26). To test whether this effect was detectable in our *EST2* expression system, laboratory *est2⁻ rad52⁻* and *est2⁻ mre11⁻* mutants (created by Hiranthi Thambugala and Brian Wasko) were analyzed using the plate senescence assay. Interestingly, the senescence streak assay confirmed that strains containing either *RAD52* or *MRE11* inactivated in the telomerase-deficient strain ($\Delta est2$ -BY4742) senesced earlier (3 streaks) than the normal telomerase-deficient strain that senesced in four streaks as before (Figure 12). The *rad52⁻ est2⁻* mutants senesced on the 3rd streak while *mre11⁻* mutants began senescing on the 2nd streak. Based on these mutants' loss of gene function and early senescence, this assay was applicable to testing senescence with other mutant strains lacking important genes necessary for DNA stability.

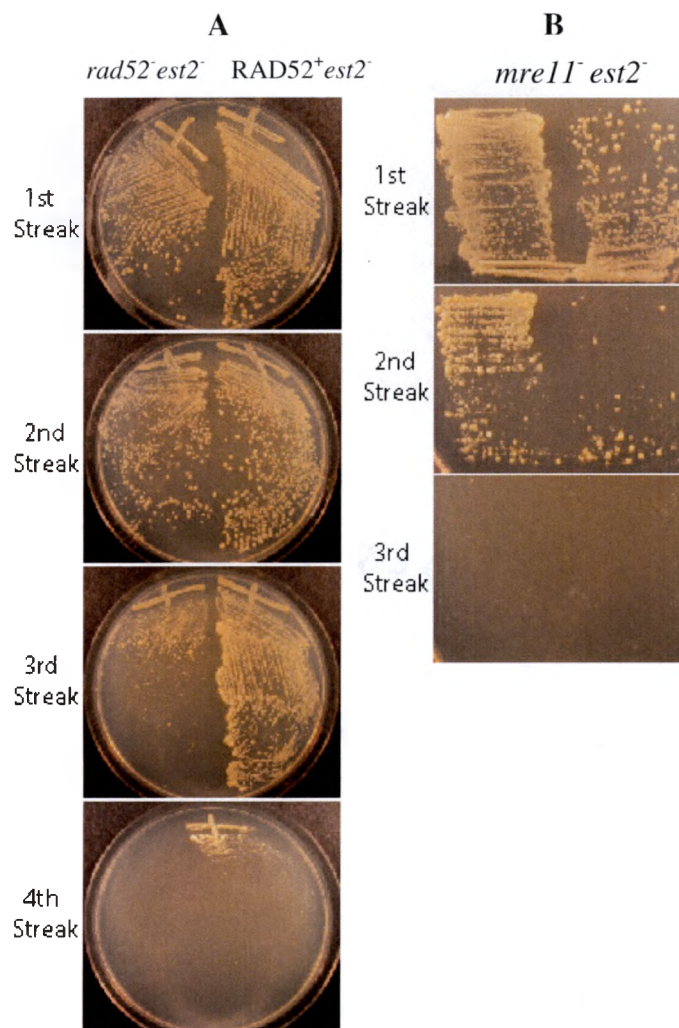


Figure 12. (A) *est2⁻ rad52⁻* and control *est2⁻ RAD52⁺* cells grown on Glu-Ura plates (*EST2* not expressed), (B) *est2⁻ mre11⁻* cells grown on Glu-Ura plates.

In yeast cells, a common method for inactivating genes is to perform a gene disruption, involving replacement of a gene's coding region with that of another gene by recombination. Nearly all DNA recombination in yeast is homologous and therefore inactivating a gene encoding a protein or enzyme can be done in one or two steps (41). A target gene, such as *GPX3* shown in Figure 13, has been interrupted by a selectable marker, *G418^r* in this example. After transformation of a DNA fragment containing the

marker gene *G418^r* flanked by portions of the 5' and 3' end of *GPX3*, homologous recombination between the ends of this DNA fragment replaces the chromosomal *GPX3* gene with the marker gene, *G418^r*. This procedure is performed by using PCR fragment-mediated gene disruption and allows production of mutant strains to further ones' studies. Most cells that have become resistant to the antibiotic G418 have had the marker gene inserted into *GPX3*, though occasionally the marker has inserted itself at another location in one of the 16 yeast chromosomes. To confirm correct gene disruption, genomic DNA from independent G418-resistant transformants is purified and tested. The test is performed by PCR using new primers from outside the *GPX3* gene coding region (shown as 5' *GPX3* and 3' *GPX3* primers in Figure 13). The PCR product obtained from the normal *GPX3* gene will be a different size from the product after insertion of *G418^r* and can be detected on a gel.

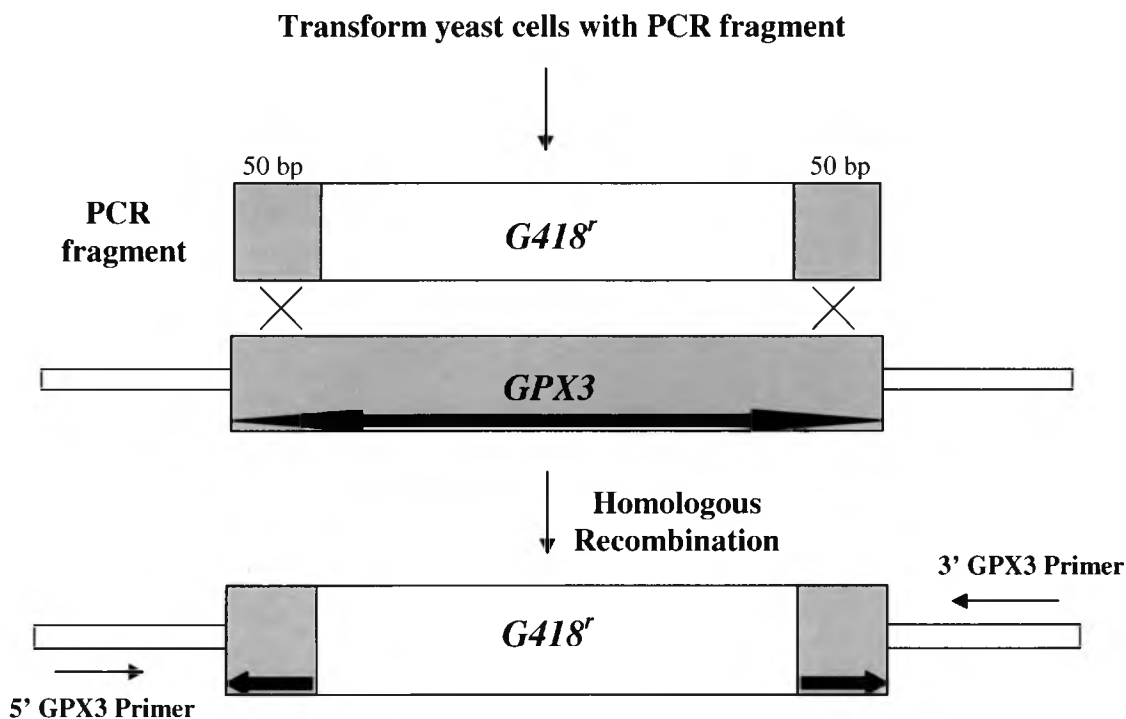


Figure 13. Chromosomal *GPX3* gene disruption by homologous recombination.

Analysis of growth potential of antioxidant mutant cells via senescence plate assays

Even though increased levels of oxidation caused by pro-oxidant chemicals did not have strong effects on senescence it is possible that other approaches might be more successful at revealing potential influences of oxidation on this process. Cells can respond to oxidative damage via several antioxidant defense mechanisms. Enzymes such as superoxide dismutase (SOD), catalase, glutathione peroxidase (GPX) and antioxidants glutathione (GSH) plus vitamins C and E are effective defense mechanisms against reactive oxygen species (ROS). These antioxidant enzymes are effective in combating ROS and preventing them from inducing damage to the cell membrane and chromosomal DNA. The antioxidant enzymes mentioned above catalyze specific reactions and in the process minimize levels of oxidation (Figure 14). As shown in Figure 14-A and B, SOD and catalase work sequentially to convert superoxide radicals to molecular oxygen and water. Figure 14-C illustrates the free radical inactivating ability of glutathione (GSH) and also glutathione peroxidase.

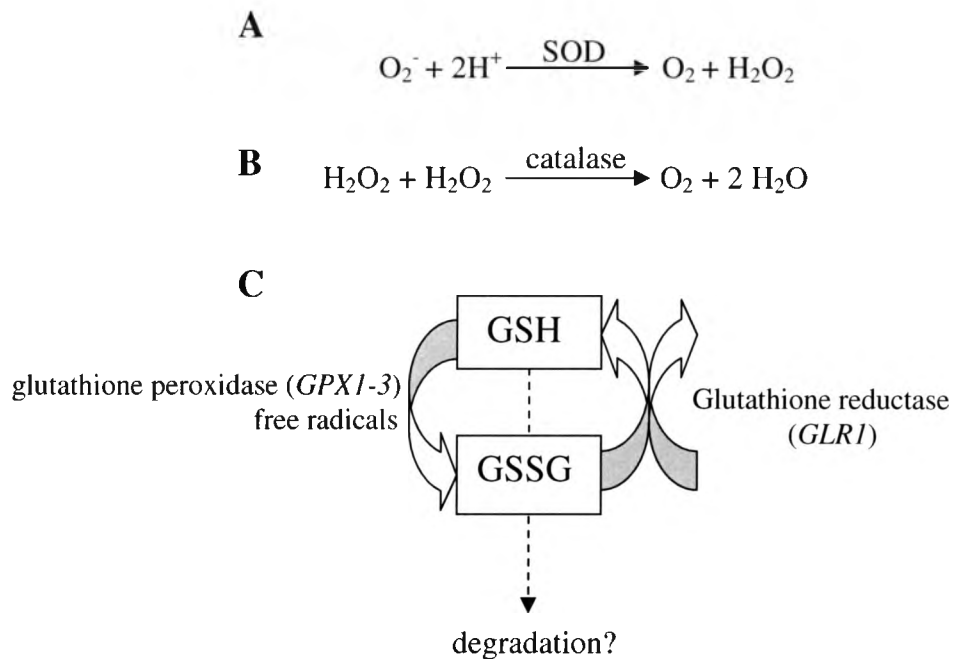


Figure 14. (A) Superoxide dismutase catalyzes the cleavage of superoxide. (B) Catalase is a second defense that catalyzes the inactivation of hydrogen peroxide. (C) The yeast glutathione cycle. GSH is oxidized to GSSG by reaction with free radicals or in reactions catalyzed by Gpx1-3. GSH is regenerated in a NADPH-dependent reaction catalyzed by Glr1.

This project focused initially on the latter two antioxidant enzymes, catalase and glutathione peroxidase. Yeast cells that lack GSH are sensitive to oxidative stress induced by oxidative radicals. *Saccharomyces cerevisiae* has three genes, *GPX1*, *GPX2* and *GPX3*, which have been proven to encode glutathione peroxidases and protect yeast against hydroperoxides during oxidative stress. Evidence suggests that *GPX3* is more important than the other two forms of the enzyme (3). In the *S. cerevisiae* genome, two genes have been identified that encode catalase enzymes, *CTT1* and *CTA1*. To observe the phenotype of cells lacking the major forms of glutathione or catalase, the first goal

was to inactivate the genes encoding these enzymes. The ultimate question was whether inactivation of these enzymes would accelerate senescence in cells that do not express telomerase, possibly by accelerating telomere shortening. The normal chromosomal *GPX3* and *CTT1* genes were therefore inactivated separately to begin this project. The agarose gel in Figure 15 is an example of a *G418^r* resistance gene fragment that was amplified via PCR from the plasmid pFA6MX4 using primers gGPX3a and gGPX3b. The primers gGPX3a and gGPX3b each have 50 nucleotides of sequence on their ends that is identical to the 5' and 3' ends of the *GPX3* gene. Thus, their PCR product has the *G418^r* marker gene plus flanking *GPX3* homology that can recombine *in vivo* with the normal *GPX3* gene for replacement. Similarly, *G418^r* on the plasmid pFA6MX4 was separately amplified using primers gCTT1a and gCTT1b to begin creating an antioxidant mutant lacking *CTT1*.

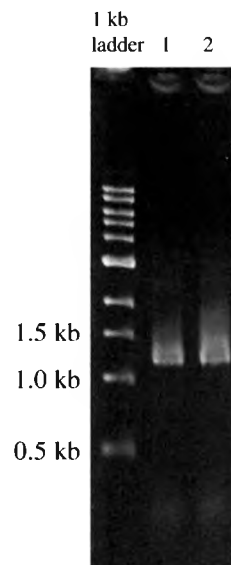


Figure 15. PCR amplification of the *G418^r* gene from plasmid pFA6MX4 using primers gGPX3a and gGPX3b generates a 1.3 kb product (lanes 1-2). These fragments were transformed into *est2⁻*-BY4742 cells to inactivate the *GPX3* gene.

After transformation of *est2⁻*-BY4742 cells that contained the *GALI-V10p::EST2* plasmid, the GPX3a and GPX3b PCR fragment was able to integrate by homologous recombination into the *GPX3* gene locus. Cells with the correct insertion were confirmed by PCR using test primers 5' GPX3 and 3' GPX3, which anneal to sequences far outside the *GPX3* coding region (Figure 16). If the cells were inactivated accurately with the *G418^r* gene, the final PCR product for $\Delta est2 \Delta gpx3$ -BY4742 and $\Delta est2 \Delta ctt1$ -BY4742 cells is approximately 1.5 kb (lanes 2-3 and 5-8). On the other hand, the wildtype *GPX3* gene is approximately 0.8 kb (lanes 1 and 4) and the wildtype *CTT1* gene is approximately 1.9 kb (not shown). Lanes 1 and 4 indicate transformants that did not get the correct *GPX3* gene insertion.

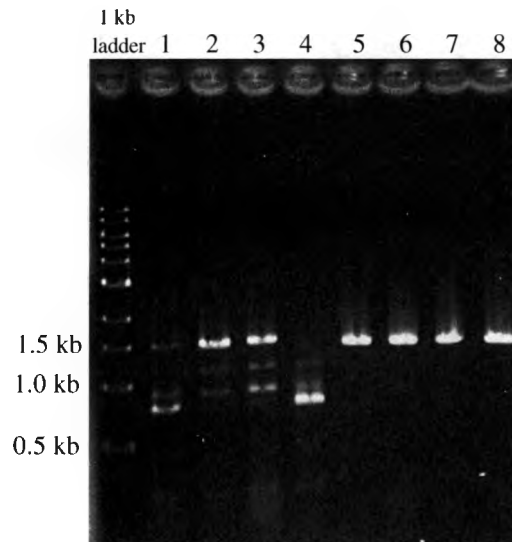


Figure 16. PCR confirmation of the *GPX3* and *CTT1* gene deletion by insertion of the *G418* resistance marker using the test primers 5'GPX3 and 3'GPX3 or 5'CTT1 and 3'CTT1. See text for lane descriptions.

The new antioxidant and telomerase-deficient strains, *est2⁻ gpx3⁻* and *est2⁻ ctt1⁻*, were tested by streaking multiple isolates (6 per plate) onto glucose plates to monitor the rate of cell senescence (Figure 17). The proposed hypothesis was that cells without a glutathione peroxidase or catalase enzyme might have high levels of DNA oxidation and undergo senescence earlier than normal *est2⁻* cells. The cells formed colonies during each of the first three streaks and by the fourth streak, all three mutant cells had undergone senescence while wildtype BY4742 cells (telomerase-proficient) continued forming colonies. The results for *est2⁻ gpx3⁻* and *est2⁻ ctt1⁻* cells did not appear any different from the *est2⁻* streak assay with regards to loss of growth during the 4th streak.

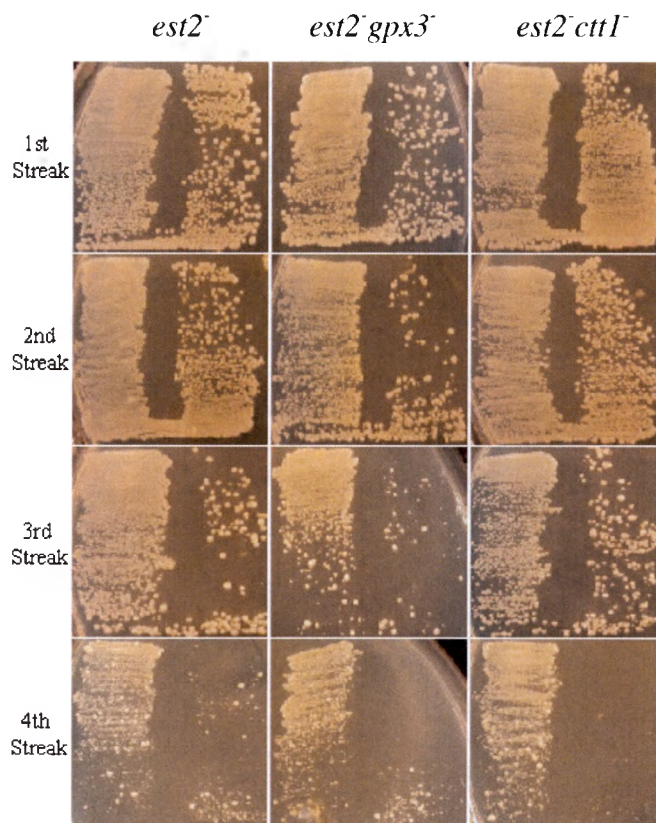


Figure 17. Mutant *est2⁻*, *est2⁻ gpx3⁻* and *est2⁻ ctt1⁻* cells were streaked onto glucose plates and incubated at 30°C.

The single antioxidant mutants demonstrated modest growth inhibition in the 3rd streak (especially *gpx3*⁻) compared to normal cells, but the timing of senescence on the 4th streak was not changed. It was hypothesized that a mutant lacking both antioxidant enzymes might have even higher levels of intracellular free radicals and therefore be more likely to influence the rate of senescence. If cells do not have both Gpx3 and Ctt1 to neutralize ROS and reduce levels of oxidation, cells will accumulate increased damage. The question is whether senescence can be accelerated in cells lacking *GPX3*, *CTT1* and *EST2*. Therefore, the same experiment was carried out in generating a mutant in the telomerase-deficient strain by inactivating both genes. The *CTT1* gene was inactivated in the $\Delta est2 \Delta gpx3$ -BY4742 strain by integrating the gene for Nat1 (nourseothricin) resistance into the *CTT1* gene locus by homologous recombination. The cells that were inactivated accurately with the *Nat1*^r gene were streaked onto glucose plates along with controls to investigate whether senescence was affected at 30°C (Figure 18-A). Cells grew at near normal rates compared to normal telomerase-deficient cells and antioxidant mutants with only one gene (either *GPX3* or *CTT1*) inactivated. The newly developed antioxidant double mutants did not strongly affect the rate of telomere shortening at 30°C. Because oxidation reactions are generally increased at higher temperatures, additional experiments were done to test the possibility that *CTT1* and *GPX3* inactivation might have greater effects at elevated temperatures. This hypothesis was correct because growth of the mutant cells was inhibited at 40°C on the 3rd streak (Figure 18-B) compared to the 4th streak during normal *est2*⁻ growth. Thus, at elevated temperatures, *est2*⁻ *gpx3*⁻ *ctt1*⁻ mutants are sensitive and senesce on the 3rd streak.

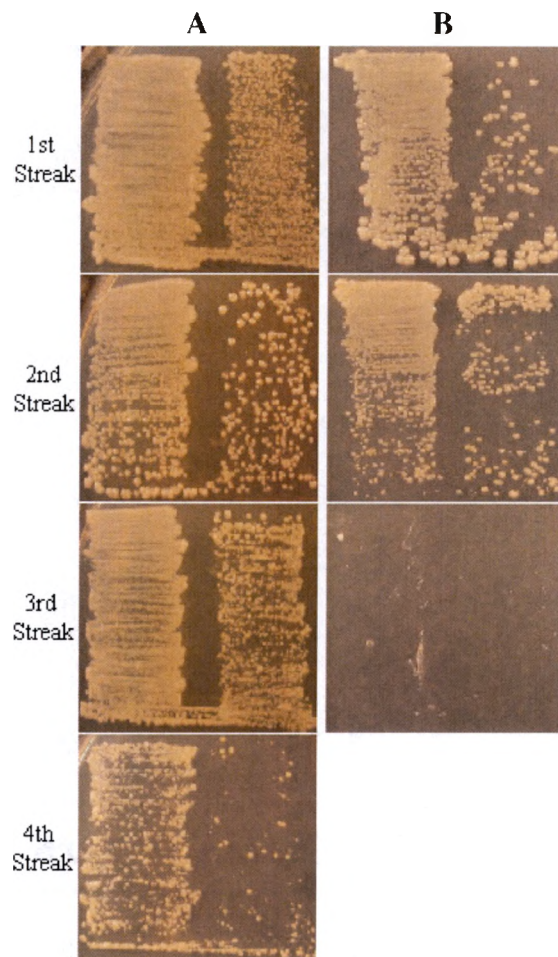


Figure 18. *est2⁻ gpx3⁻ ctt1⁻*-BY4742 cells streaked on glucose plates every three days and incubated at (A) 30°C or (B) 40°C.

Many additional genes have been identified in eukaryotes that affect cellular resistance to oxidative damage. Since the susceptibility of cellular DNA to oxidation may depend on both the nature and amount of free radicals, other gene mutants were tested. The following series of senescence assays were optimized based on experience with the preliminary antioxidant mutant studies. For the next experiments, several mutant strains were obtained from Simon Avery's lab at the University of Nottingham with multiple genes encoding glutathione peroxidase enzymes and a Yap1 transcription

factor inactivated in the parent strain BY4741. Yap1 is a transcription factor that has been implicated in oxidative stress responses in yeast (30). Under stressful oxidative conditions, the expression of several antioxidant genes is up-regulated by Yap1. Specifically, Yap1 controls the expression of *GSH1* and *GLR1* and cooperates with Skn7 to control expression of *TRX2* and *TRR1*. Lee *et al.* reported that strains with either Yap1 or Skn7 inactivated are hypersensitive to H₂O₂ (26). In addition to *yap1⁻* and *yap1⁻gpx3⁻* strains, a *gpx3⁻gpx2⁻gpx1⁻* triple mutant was also investigated. Initially, strains were transformed with the plasmid pLKL82Y (*GALI-V10p::EST2 URA3*). The chromosomal copy of the *EST2* gene was then inactivated via homologous recombination to allow modulation of senescence by regulated expression of the plasmid *EST2* gene. The parent strain BY4741 was also transformed with pLKL82Y and chromosomal *EST2* was inactivated to have a control using the *EST2* system but without any antioxidant genes inactivated. Senescent streak assays were performed by comparing multiple isolates of the mutant cells' growth at optimum yeast temperature (30°C) and also at a higher temperature (40°C) on glucose plates. The mutants were initially streaked onto Glu + 5-FOA plates to eliminate any possible *EST2* mutations that might allow cells to express *EST2* (only cells that have lost the *EST2⁺ URA3⁺* plasmid can grow on 5-FOA plates). All of the following streaks were done using standard synthetic glucose plates. The telomerase-deficient control BY4741 strain with no antioxidant enzymes inactivated senesced on the 5th streak when grown on both YPGlu (rich) and synthetic glucose at 30° C (Figure 19-left side). *est2⁻ yap1⁻* and *est2⁻ yap1⁻ gpx3⁻* cells also senesced on the 5th streak at 30° C. Interestingly, both the *est2⁻ yap1⁻* and *est2⁻ yap1⁻ gpx3⁻* cells formed many more large survivor mutants than normal cells (seen in the 4th streaks of Figure 19).

Importantly, at the higher incubation temperature of 40°C, *est2⁻ yap1⁻* and *est2⁻ yap1⁻ gpx3⁻* cells senesced earlier in the 4th (Figure 20). Those cells might have accumulated an increased level of oxidative damage as a consequence of a higher growth temperature (40°C).

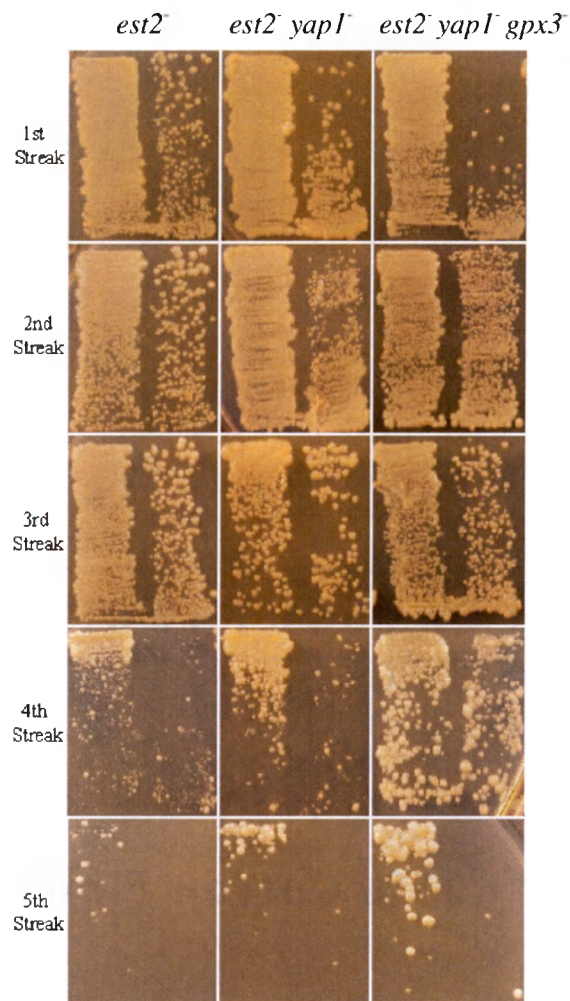


Figure 19. *est2⁻*-BY4741, *est2⁻ yap1⁻* and *est2⁻ yap1⁻ gpx3⁻* cells were streaked onto synthetic glucose plates at 30°C.

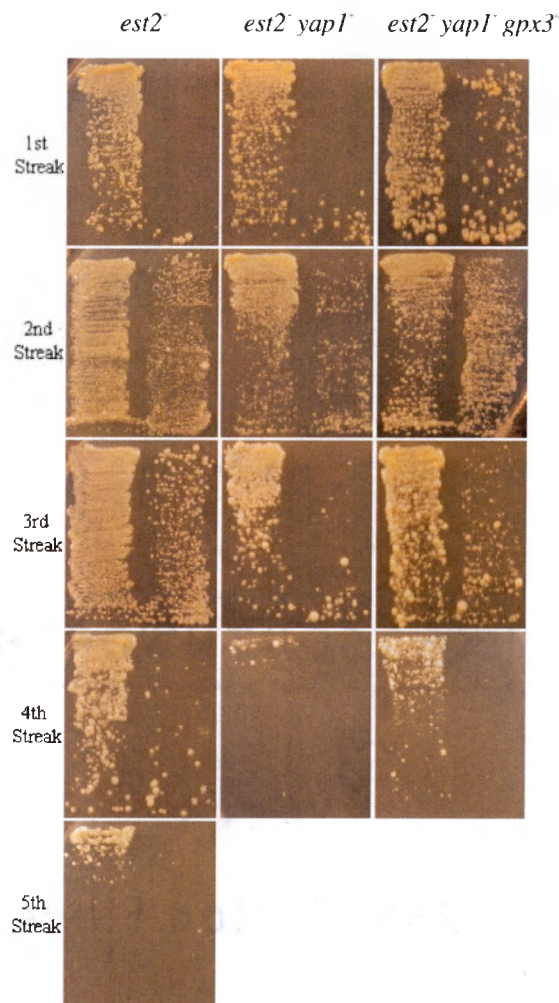


Figure 20. *est2*-BY4741, *est2 yap1* and *est2 yap1 gpx3* cells streaked on synthetic glucose plates at 40°C.

The last antioxidant strain, *est2 gpx3 gpx2 gpx1*, was also streaked under the same conditions as above, but did not senesce at 30°C (Figure 21-A and data not shown). Cells were streaked seven times previously on synthetic glucose plates, corresponding to ≥ 120 generations of growth, but senescence did not occur. It is probable that most of these cells acquired increased mutations and formed mutants that were capable of bypassing senescence. In contrast to results at 30°C, when the cells were streaked and

incubated at 40°C, most of the cells grew very poorly on the 4th and 5th streaks while others formed very large survivor mutants on the 5th streak (Figure 21-B). Thus, in strains with all three glutathione peroxidase enzymes inactivated (*GPX3*, *GPX2* and *GPX1*), the rate of senescence at higher temperatures was modestly accelerated, though not as strongly as with the *yap1* strains.

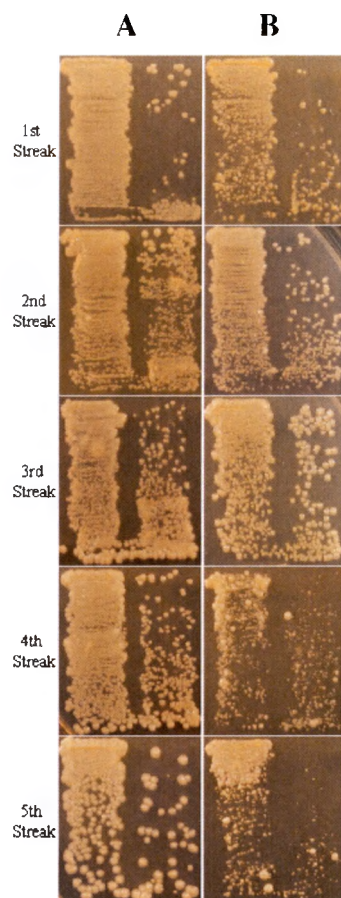


Figure 21. *est2 gpx3 gpx2 gpx1* cells streaked on glucose plates at (A) 30°C or (B) 40°C.

The results obtained from these antioxidant mutant senescence assays suggest that the role of Yap1 is significant in cells lacking telomerase. Experiments discussed

previously suggest that oxidation may play a role in the rate of telomere shortening, but the precise mechanism by which telomere shortening ultimately leads to senescence is still unknown.

Testing senescence models: does reactivation of telomerase in late senescence rescue cells that have lost the ability to grow?

There are four models that have been proposed to explain why telomere shortening leads to cellular senescence. One model suggests that uncapping of telomeres leads to the formation of lethal end-to-end fusions and other chromosome rearrangements that ultimately cause cells to senesce (28, 42, 43, 44, 45). End-to-end fusions create dicentric chromosomes which result in two centromeres being pulled apart during mitosis leading to chromosome breakage and cell death. Another model proposes that an exonucleolytic end resection mechanism is responsible for initiating chromosome instability at shortened telomeres and digestion of DNA at ends ultimately results in deletion of essential genes (44). When the ends of chromosomes have lost most proteins forming the telomere cap, the ends are not only exposed to chromosome rearrangements and fusions, but are exposed to exonucleases, such as Exo1 found in yeast. Digestion by Exo1 is an intermediate step in senescence and can involve removal of thousands of nucleotides from the ends (28), including possibly the subtelomeric region and essential coding regions of genes. A third model suggests that cells are programmed to die and ultimately commit suicide (apoptosis) and therefore senesce (43). Although not a frequently cited model, it remains possible that cells respond to the shortened telomeres by halting growth (mostly in G₂ phase) without dying immediately. In this model,

senescence is reversible and although cells have arrested growth, they are not absolutely destined to die.

The *GALI-VI0::EST2* regulatory system used in these experiments allows for testing the models because it is possible to allow senescing cells to grow in glucose until cells stop growing. These late senescent cells can then be switched onto galactose media to turn on the *GALI-VI0p::EST2* fusion, reactivating telomerase expression. If senescence is reversible, then the Est2 polymerase will replenish the ends of the chromosomes and cells will resume growing. These assays were initially conducted with *est2⁻* cells. The cells were streaked from a fresh Gal-Ura plate onto a Glu-Ura plate for the first streak and were incubated at 30°C for three days. Individual colonies were selected and restreaked onto fresh Glu-Ura plates for a second, third, and fourth streak. The third streak was grown for four days before harvesting seven isolated colonies that were then diluted, sonicated and counted using a hemacytometer to measure total cells in the culture. Aliquots were spread onto Glu-Ura and Gal-Ura plates and incubated for three days to determine the fraction of cells that could still form colonies. The plating efficiency on glucose was, as expected, very low ($0.7\% \pm 0.31\%$). This compares to normal BY4742 cells (*EST2⁺*), which have a plating efficiency of approximately 70%. In contrast, when senescent cells were spread onto galactose, which results in reactivation of *EST2* expression, the plating efficiency was $30.8\% \pm 6.6\%$. This represents a 44-fold increase.

Aliquots of cells from a 4th plate streak were also harvested and spread onto Glu-Ura and Gal-Ura plates and incubated for three days. The plating efficiency on glucose was $0.04\% \pm 0.06$. In contrast to glucose, when cells were spread onto galactose the

plating efficiency was $7.9\% \pm 4.2\%$. This represents a 197-fold increase. These results suggest that most cells seemingly on the brink of death (i.e., they were completely unable to grow) could be rescued if telomerase extended their shortened telomeres. The results are inconsistent with the first three previously mentioned models of senescence proposing that telomere shortening is irreversible, e.g., apoptosis, formation of lethal chromosome fusions, or deletion of essential genes from the ends.

Another experiment, similar to the *est2⁻* reactivation assays, was conducted with *est2⁻ rad52⁻* mutant cells to compare rescue ability of these senescent cells on galactose and glucose to the original *est2⁻* reactivation. The double mutant, *est2⁻ rad52⁻*, had a more severe growth defect than *est2⁻* mutants. After *est2⁻ rad52⁻* mutant cells were streaked for the third streak and grown for 4 days, seven isolated colonies were diluted, sonicated and counted similar to the initial reactivation experiment. Aliquots were spread onto Glu-Ura and Gal-Ura plates and incubated for three days. The plating efficiency on glucose was $0.003\% \pm 0.001\%$. However, when cells were spread onto galactose, which results in reactivation of *EST2* expression, the plating efficiency was $8.0\% \pm 6.7\%$ (2700-fold higher than glucose). *RAD52* has been shown to be involved in homologous recombination in maintaining telomere lengths (26). Therefore, senescing cells survive longer if homologous recombination is proficient, i.e., if cells do not express *RAD52*, they will die at an increased rate compared to normal *est2⁻* mutants.

The *EST2* reactivation experiments indicate that the process of senescence is strongly reversible even in the latest stages of cellular senescence. Put another way, the results have also implied that although the cells are no longer dividing, after ~ 60-70 generations, they are still alive. An experiment was performed to estimate how long

senescence remained reversible. Initially, the holding experiment was conducted to determine if cells do eventually lose the ability to be rescued and secondly, if changes in the ability to rescue senescent cells occur suddenly or slowly. To begin this experiment, *est2⁻* cells were streaked from a fresh Gal-Ura plate onto a Glu-Ura plate for the first streak and were incubated at 30°C for three days. After the second streak, individual colonies were diluted, sonicated, counted in the hemacytometer and spread to Glu-Ura plates for the third spread (similar to a third streak). Three days later, seven isolated colonies were harvested and the same plates were placed back into the 30°C incubator for two more days. Seven colonies were harvested every second day for a total of eight consecutive days. Aliquots were spread onto Glu-Ura and Gal-Ura plates and incubated for three days. The plating efficiency (P.E.) for the first post-senescent spread (after 60-80 generations) onto glucose was 0.64 % \pm 0.57%. In contrast, when cells were spread onto galactose, which results in reactivation of *EST2* expression, the P.E. was 36.0 % \pm 17.0 %, a 56-fold increase. The reversibility of senescence remained relatively high for a long time. As shown in Figure 22 after approximately 60 generations plus additional incubation for 2, 4 or 6 days at 30°C, *est2⁻* cells could still be rescued when spread onto galactose and were not dying suddenly, but slowly. Although the standard deviation variability was large in the individual assays, standard deviation of the plating efficiencies never overlapped and even after eight days, survival on galactose was ten fold higher than on glucose (Figure 22).

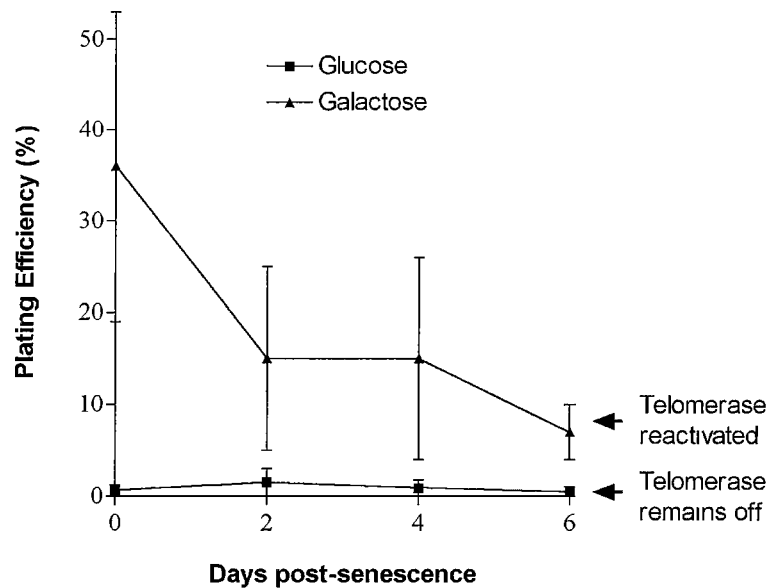


Figure 22. Plating efficiency of *est2*⁻ cells during the holding experiment. The zero time point corresponds to approximately 60 generations of growth (3 plate streaks), when most cells have stopped growing.

As mentioned previously, the last model has proposed that cells respond to shortened telomeres by halting growth and pausing in G₂ phase of the cell cycle. When cells have accumulated DNA damage, cells will pause in G₂ phase to repair any damage before entering mitosis. The cell cycle checkpoint regulatory genes *MEC3* and *RAD24* are required for cells to arrest in G₂ after accumulating DNA damage. These checkpoint genes, *MEC3* and *RAD24*, were inactivated in telomerase-deficient (*est2*⁻-BY4742) cells and the question is whether they can continue to pause in the G₂ phase and if they can be rescued like checkpoint-proficient cells. If cells cannot arrest and repair damage in G₂ it is likely that the reversibility of senescence will be altered in telomerase-deficient cells.

Future studies will involve performing senescence streaks and reactivation experiments to compare these checkpoint mutants with normal cells.

Summary

In summary, this research project has successfully characterized several nutritional and environmental parameters that affect the rate of telomere shortening. This was accomplished by using the *EST2* expression system initially to establish optimum growth on various sugar concentrations and at various growth temperatures. Several pro-oxidants and antioxidant enzymes were investigated to monitor effects of increased oxidation on the rate of senescence. The latter part of this project began investigating the models proposed to explain why telomere shortening leads to cell death.

When telomerase-deficient cells are calorie restricted from the normal 2.0% glucose to 0.02% glucose, cells appeared to grow normally and generated fewer survivor mutants. However, when *est2⁻* cells were grown on 8.0% glucose, it appeared that they did not go through as many generations and had a stronger killing by the 4th streak. Although this data does not support that lifespan can increase by caloric restriction, it suggests that a one hundred fold decrease in the normal caloric intake does not affect senescence and decreases the rate of survivor mutations.

Several pro-oxidants were investigated and some of those demonstrated modest effects on senescence. Interestingly, at two high doses of tert-butyl hydroperoxide (0.5 mM and 0.75 mM), growth of wildtype cells was more inhibited than telomerase-deficient cells on the 1st streak. However, when both wildtype and telomerase-deficient cells were streaked onto 0.25 mM t-BHP, telomerase-deficient cells senesced in the normal four streaks. This effect is being further investigated. Menadione and cadmium, as well as the other pro-oxidants, iron and H₂O₂, did not have strong effects on the rate of telomere shortening. The pro-oxidant results suggest that induced oxidation in yeast cells

does not influence the rate of senescence. If senescence is not altered under increased levels of pro-oxidants, could it be affected in cells lacking the enzymes necessary to neutralize and/or reduce reactive oxygen species? Several antioxidant mutants were created to test whether senescence is accelerated in cells lacking Gpx3, Gpx2, Gpx1, Ctt1 and/or the Yap1 transcription factor. A double mutant, *gpx3⁻ ctt1⁻*, demonstrated accelerated senescence at an elevated temperature of 40°C. *yap1⁻* and *yap1⁻ gpx3⁻* mutants also senesced earlier than normal *est2⁻* cells at elevated temperatures. On the other hand, a mutant lacking all three glutathione peroxidase enzymes accumulated survivor mutants at a higher frequency at 30°C compared to the other two mutants mentioned before. These mutants suggest that elevated levels of oxidation can play a role in the rate of cellular senescence.

If the major cause of senescence is degradation of chromosome ends that can further generate end-to-end fusions and rearrangements, then reactivation of telomerase should not have rescued cells that had lost the ability to grow. The same logic applies to two other models. If apoptosis or loss of essential genes by exonuclease activity were correct, then cells could not have been rescued by extending shortened telomeres. This research project partially supports the last model proposing that cells are alive, but have halted growth and are simply no longer progressing through the cell cycle. Data from the holding experiment supports this theory, suggesting that senescence is reversible and telomerase can be reactivated in cells well after 60-80 generations of growth. The exact cause of loss of growth and cellular senescence is still to be determined, but these experiments have cast some doubt on the major model (end-to-end fusions) and suggest that future studies must consider the possibility that other mechanisms may be involved.

REFERENCES

1. Hahn, W.C. Myerson, M. *Ann Med.* **2001**, 33, 123-129.
2. Rowley, P.T. Tabler, M. *Anticancer Res.* **2000**, 20, 4419-4429.
3. Grant, C.M. *Molecular Microbiology.* **2001**, 39, 533-541.
4. Meeker, A.K.; Hicks, L.J.; Platz, E.A.; March, G.E.; Bennett, C.M.; Delannoy, M.J.; de Marzo, A.M. *Cancer Res.* **2002**, 62, 6405-6419.
5. Mathon, N.F.; Lloyd, A.C. *Nat Rev Cancer.* **2001**, 1, 203-213.
6. Rudolph, K.L.; Chang, S.; Lee, H.W.; Blasco, M.; Gottlieb, G.J.; Greider, C.; DePinho, R.A. *Cell.* **1999**, 96, 701-712.
7. Mondello, C.; Scovassi, A.I. *Biochem Cell Biol.* **2004**, 82, 498-507.
8. Mukherjee, A.B.; Costello, C. *Mech Ageing Dev.* **1998**, 103, 209-222.
9. Wong, K.K.; Chang, S.; Weiler, S.R.; Ganesan, S.; Chaudhuri, J.; Zhu, C.; Artandi, S.E.; Rudolph, K.L.; Gottlieb, G.J.; Chin, L.; Alt, F.W.; DePinho, R.A. *Nat Genet.* **2000**, 26, 85-88.
10. Cawthon, R.M.; Smith, K.R.; O'Brien, E.; Sivatchenko, A.; Kerber, R.A. *Lancet.* **2003**, 361, 393-395.
11. Davenport, R.J. *Sci. Aging Knowl. Environ.* **2005**, 2005, (16) pp. nf31.
12. Dugan, L.L.; Quick, K.L. *Sci. Aging Knowl. Environ.* **2005**, 2005, (26) pp. pe20.
13. Brozmanova, J.; A. Dudas; J.A. Henriques. *Neoplasma.* **2001**, 48, 85-93.
14. Beckman, K.B.; Ames, B.N. *Phys Rev.* **1998**, 78, 547-581.
15. Oikawa, S.; Kawanishi, S. *FEBS Let.* **1999**, 453, 365-368.
16. Chen, Q.; Fischer, A.; Reagan, J.D.; Yan, L.; Ames, B.N. *Proc. Natl. Acad. Sci.* **1995**, 92, 4337-4341.

17. Brennan, R.J.; Schiestl, R.H. *Mutation Research*. **1996**, 356, 171-178.
18. Melov, S.; Ravenscroft, J.; Malik, S.; Gill, M.S.; Walker, D.W.; Clayton, P.E.; Wallace, D.C.; Malfroy, B.; Doctrow, S.R.; Lithgow, G.J. *Science*. **2000**, 289, 1567-1568.
19. Orr, W.C.; Sohal, R.S. *Science*. **1994**, 263, 1128-1130.
20. Grant, C.M.; Perrone, G.; Dawes, I.W. *Biochemical and Biophysical Research Communications*. **1998**, 253, 893-898.
21. Furumoto, K.; Inoue, E.; Nagao, N.; Hiyama, E.; Miwa, N. *Life Sci*. **1998**, 63, 935-948.
22. Della Croce, C.; Bronzetti, G.; Cini, M.; Caltavuturo, L.; Poi, G. *Toxicol In Vitro*. **2003**, 17, 753-759.
23. Lundblad, V. *Oncogene*. **2002**, 21, 522-531.
24. Zhou, J.; Hidaka, K.; Futcher, B. *Mol Biol Cell*. **2000**, 20, 1947-1955.
25. Grandin, N.; Damon C.; Charbonneau, M. *EMBO Journal*. **2001**, 20, 6127-6139.
26. Le, S.; Moore, J.K.; Haber, J.E.; Greider, C.W. *Genetics*. **1999**, 152, 143-152.
27. Enomoto, S.; Glowczewski, L.; Berman, J. *Mol Biol Cell*. **2002**, 13, 2626-2638.
28. Ijima, A.S.; Greider, C.W. *Mol Biol Cell*, **2003**, 14, 987-1001.
29. Manfredini, V.; Roehrs, R.; Peralba, M.C.R.; Henriques, J.A.P.; Saffi, J.; Ramos, A.L.L.P.; Benfato, M.S. *Braz J Med Biol Res*. **2004**, 37, 159-165.
30. Maeta, K.; Izawa, S.; Okazaki, S.; Kuge, S.; Inoue, Y. *Mol Biol Cell*. **2004**, 24, 8753-8764.
31. Chae, H.Z.; Kim, I.; Kim, K.; Rhee S.G. *J Biol Chem*. **1993**, 268, 16815-16821.
32. Brachmann, C.B.; Davies, A.; Cost, G.J.; Caputo, E.; Li, J.; Hieter, P.; Boeke, J.D. *Yeast*. **1998**, 14, 115-116.
33. Avery, A.M.; Willets, S.A.; Avery, S.V. *Journal of Biol Chem*. **2004**, 279, 46652-46658.
34. Gietz, R.D.; Schiestl, R.H.; Willems, A.R.; Woods, R.A. *Yeast*. **1995**, 11, 355-360.

35. Soni, R.; Carmichael, J.P.; Murray, J.R. *Curr Genet.* **1993**, 24, 455-459.
36. Lewis, L.K.; Kirchner, J.M.; Resnick, M.A. *Mol Cell Biol.* **1998**, 18, 1891-1902.
37. Thambugala, H. *Use of a New Regulatable Telomerase Expression System to Monitor In Vitro Cell Aging and the Effects of DNA Damage on Replicative Senescence*, Master's Thesis. **2005**, 10-20.
38. Koppenol, W.H. *Free Radical Damage and its Control.* **1994**, 28, 3-24.
39. Chaudiere, J. *Free Radical Damage and its Control.* **1994**, 25-66.
40. Okayasu, H.; Ishihara, M.; Satoh, K.; Sakagami, H. *Anticancer Res.* **2001**, 21, 2387-2392.
41. Johnston, M.; Riles, L.; Hegemann, H. *Methods Enzymology.* **2002**, 350, 290-311.
42. Ducray, C.; Pommier, J.P.; Martins, L.; Boussin, F.D.; Sabatier, L. *Oncogene.* **1999**, 18, 4211-4223.
43. Hayflick, L. *Exp Gerontol.* **2003**, 38, 1231-1241.
44. Hackett, J.A.; Feldser, D.M.; Greider, C.W. *Cell.* **2001**, 106, 275-286.
45. van Steensel, B.; Smogorzewska, A.; de Lange, T. *Cell.* **1998**, 92, 401-413.

VITA

Alison Lee Russell was born in Houston, Texas on June 11, 1980, the daughter of Lee Russell and Nancy W. Russell. After completing her work at Harlingen High School South, Harlingen, Texas, in 1999, she entered Baylor University, Waco Texas. She received the degree of Bachelor of Science from Baylor University in December 2003. During the following spring she entered the University of Texas at San Antonio. In August 2004, she entered the Graduate College of Texas State University-San Marcos.

Permanent Address: 26163 Altas Palmas Rd
Harlingen, Texas 78552

This thesis was typed by Alison Lee Russell

